Matthias Piffl, BSc

Reaktionen von Methanol auf sehr dünnen Pd/Zn- und Pd/ZnO-Oberflächen

MASTERARBEIT

zur Erlangung des akademischen Grades
Diplom-Ingenieur

Masterstudium Technische Physik

Technische Universität Graz

Betreuer:

Ao. Univ. Prof. Mag. Dr. rer. nat. Robert Schennach

Institut für Festkörperphysik

Graz, August 2011

Matthias Piffl, BSc

Reactions of methanol on ultra-thin Pd/Zn- and Pd/ZnO- surfaces

MASTER THESIS

For obtaining the academic degree
Diplom-Ingenieur

Master Programme of
Technical Physics

Graz University of Technology

Supervisor:

Ao. Univ. Prof. Mag. Dr. rer. nat. Robert Schennach

Institute of Solid State Physics

Graz, August 2011

Deutsche Fassung:
Beschluss der Curricula-Kommission für Bachelor-, Master- und Diplomstudien vom 10.11.2008
Genehmigung des Senates am 1.12.2008

EIDESSTATTLICHE ERKLÄRUNG

Ich erkläre an Eides statt, dass ich die vorliegende Arbeit selbstständig verfasst, andere als die angegebenen Quellen/Hilfsmittel nicht benutzt, und die den benutzten Quellen wörtlich und inhaltlich entnommene Stellen als solche kenntlich gemacht habe.

Graz, am …… ……..
(Unterschrift)

Englische Fassung:

STATUTORY DECLARATION

I declare that I have authored this thesis independently, that I have not used other than the declared sources / resources, and that I have explicitly marked all material which has been quoted either literally or by content from the used sources.

…… ……..
date (signature)

Acknowledgements

First of all, I would like to thank my Professor and supervisor, Robert Schennach, whose encouragement, supervision and support from the experimental to the theoretical stage enabled me to develop my master thesis in the present quality.

I would like to express my gratitude to my colleague and friend, Frederik Weber, who worked with me on various experiments, supported me in so many ways and always had a sympathetic ear for my concerns.
In addition I want to thank Martin Kornschober for all his technical drawings and his great doings on fulfilling all our complex technical wishes.

My special thanks go to Professor Adolf Winkler who was always available for a piece of advice.

Furthermore I wish to express my deepest gratitude to the Technical University of Graz, the Institute of Solid State Physics as well as the FWF Wissenschaftsfond for funding this project. Without their support none of the experiments within this thesis would have been possible and I am really thankful for that!

Last but not least I would like to thank those who supported me in my private life: My mother and my father who gave me the most unique support through all the years, my brother who constantly reminded me of important deadlines and my wife who is simply amazing.
A little note to my son, although many years will pass until he can read this: Thanks for distracting me at all the right moments and motivating me with your little smile.

Abstract

This diploma serves to better understand the catalytic processes which are found on Pd/ZnO layers. Catalysts of this type are used in direct methanol fuel cells to be able to use the bound hydrogen in the fuel cell. Methanol desorption from Pd/Zn and Pd/ZnO was investigated by thermal desorption spectroscopy (TDS) and reflection absorption infrared spectroscopy (RAIRS).
Experiments with Zn and ZnO layers thicknesses between 1.4 and 0.04 ML were done. Also the amount of methanol dosed on the sample surface was varied. However, no significant differences of measured desorption products and their desorption temperatures were found at various layer thicknesses.
Furthermore, the influence of the oxygen pressure during Znic exposure on the desorption temperature of the reaction products of methanol was examined. The oxygen pressure is responsible for the ZnO structure formed on the sample surface. Large differences between partly and fully oxidized ZnO surfaces were found especially in the temperature range above 300 K.
RAIRS measurements confirm the data obtained by TD-spectroscopy, although a layer thicknesses of less than one half of a monolayer ZnO leads to a significant decrease of relevant peaks measured.
Due to the high complexity of the entire system no exact statements regarding the reaction pathways could be done. Therefore, further investigations are needed to be able to understand them in more detail.

Zusammenfassung

Diese Diplomarbeit dient dem besseren Verständnis der katalytischen Prozesse, die auf Pd/ZnO Schichten vorzufinden sind. Katalysatoren dieser Art werden in Direkt-Methanol-Brennstoffzellen verwendet, um den in Methanol gebundenen Wasserstoff für die Brennstoffzelle nutzbar zu machen. Methanoldesorption von dünnen und ultra-dünnen Pd/Zn und Pd/ZnO Schichten wurde mittels Thermodesorptionsspektroskopie (TDS) und Reflektions-Absorption-Infrarot-Spektroskopie (RAIRS) untersucht.
Es wurden Experimente mit Zn- und ZnO- Schichtendicken zwischen 1.4 und 0.04 ML durchgeführt, wobei auch die auf die Probe aufgetragene Menge an Methanol variiert wurde. Es konnten jedoch keine signifikanten Unterschiede bei verschiedenen Schichtdicken sowie der gemessenen Desorptionsprodukte und ihren Desorptionstemperaturen gefunden werden.
Auch der Einfluss des Sauerstoffdrucks auf die Desorptionstemperatur der Methanolreaktionsprodukte während der Zink Bedampfung wurde untersucht. Dieser ist verantwortlich für die ZnO Struktur, die sich auf der Probenoberfläche bildet. Dabei wurde festgestellt, dass speziell im Temperaturbereich über 300 K große Unterschiede zwischen stark und schwach oxidierten ZnO-Flächen zu finden sind.
Die RAIRS Messungen bestätigen die durch TD-Spektroskopie erhaltenen Daten, obwohl im Bereich unter eines halben Monolayers ZnO die Anzahl an relevanten Peaks stark abnimmt.
Aufgrund der hohen Komplexität des gesamten Systems konnten leider keine genauen Aussagen über die Reaktionswege gefunden werden. Daher sind weitere Untersuchungen notwendig um diese im Detail verstehen zu können.

Contents

1. Motivation

Alternative resources instead of fossil fuel become more and more important. These days hydrogen offers a clean alternative but pure hydrogen is difficult to store. Its boiling point is 20.28K and its atomic radius is so small that single atoms can go through steel walls. There are different attempts to store hydrogen in or on a chemical carrier. A very promising carrier is Methanol (CH_3OH) which is liquid at room temperature. In this state it is easy to store and can be directly used in "Direct Methanol Fuel Cells" (DMFC). A schematic is shown in Figure 1.1 [1].

Basically a DMFC works the following way. As can be seen in Figure 1.1 a mixture of methanol and water gets injected at the anode (1.1). A catalyst disunites the hydrogen and carbon dioxide bound in methanol and water. Additionally hydrogen is separated in positively charged ions and negatively charged electrons. Hydrogen protons can get through the proton-exchange-membrane (PEM). The electrons have to go through an external circuit to compensate the lack of electrons at the cathode. While doing that they produce electric energy that can be used to power electronic equipment. But also methanol and carbon dioxide are able to pass through the membrane.
At the cathode air (oxygen, nitrogen) is supplied as the oxidant. Hydrogen protons which went through the membrane, electrons that delivered electric power and supplied oxygen react to water (1.2). Methanol that reaches the cathode reacts with oxygen to water and carbon dioxide. The overall reaction is described in equation (1.3). [2]

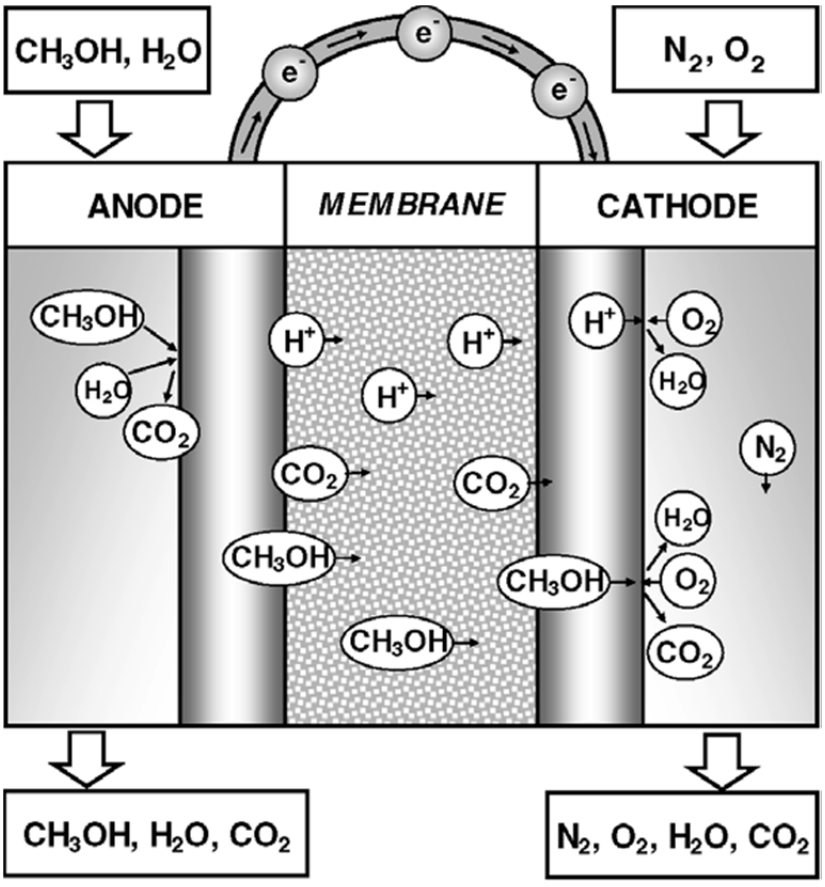

Figure 1.1: Schematic of a direct methanol fuel cell; adapted form [1].

Anode-Reaction:

$$CH_3OH + H_2O \rightarrow CO_2 + 6H^+ + 6e^- \quad \textbf{(1.1)}$$

Cathode-Reaction:

$$1{,}5O_2 + 6H^+ + 6e^- \rightarrow 3H_2O \quad \textbf{(1.2)}$$

Overall-Reaction:

$$CH_3OH + 1{,}5O_2 \rightarrow CO_2 + 2H_2O \quad \textbf{(1.3)}$$

Beside the PEM the catalyst that is able to separate methanol is the most important component. Several catalytic systems have been studied in the past few years. In the beginning cupper (Cu) on zinc oxide (ZnO) systems were used but their main problem was thermal stability. As the temperature rises, the carbon dioxide (CO_2) output gets replaced by carbon monoxide (CO) output which is poison for the fuel cell anode. Nowadays paladium (Pd) on ZnO has become the favourite substrate as the thermal stability and performance has proven to be very promising [3].

Several teams investigated the reaction mechanisms of methanol dissociation on Pd/Zn and Pd/ZnO in the last decade but they are not understood in detail yet [[3], [4], [5]]. In this master thesis TDS and RAIRS experiments with methanol decomposition on Pd(111), Pd/Zn and Pd/ZnO were done to investigate their reactivity with respect to film thickness and composition.

2. Experimental Setup

2.1. The vacuum chamber

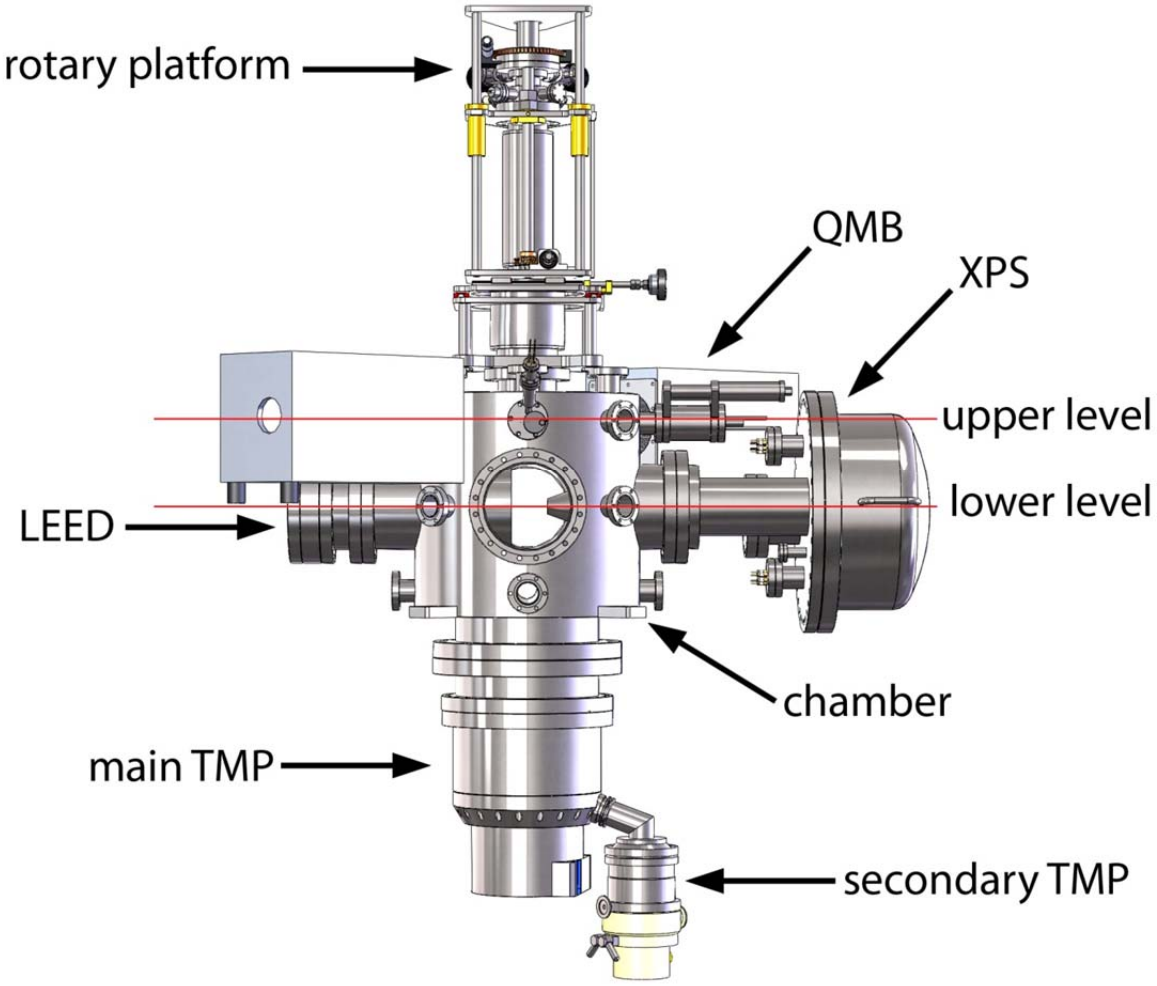

Figure 2.1: Vacuum chamber[1]

All experiments were done in an ultra-high vacuum (UHV) chamber. As the coverage time of the sample surface by residual gas is related to the pressure in the chamber, UHV is necessary to keep the sample surface clean for the time of the experiments. At a pressure smaller than 10^{-10} mbar the surface will stay clean for approximately three hours [6].

In Figure 2.1 the used UHV chamber is shown. On the top the rotary platform is seen which holds an approximately 50 cm long steel tube that extends into the chamber. On the bottom side the sample holder is mounted. The top side is open to be able to fill the tube with liquid nitrogen for sample cooling.
The rotary platform allows rotation of 340°. Additionally the whole platform can be moved 3 cm in X and Y axis and 20 cm in Z axis.

The UHV chamber has two levels (marked with red lines in Figure 2.1): Schematics are seen in Figure 2.2 (upper level), in Figure 2.3 (lower level). The distance between the two levels is

[1] Figure made by M. Kornschober

15 cm. The chamber is pumped by three turbo molecular pumps. Two turbo molecular pumps (Pfeiffer TPU 1501 P, 1450 l/s, TMP 1; Leybold Turbovac TMP 151, 145 l/s) are connected in series. This configuration has proven better performance in lowering the hydrogen pressure in the chamber than a single turbo molecular pump. The third turbo molecular pump (Pfeiffer TMU 071 P, 60l/s) is used to pump the rotary platform.
To measure the pressure in the chamber, a Bayard-Alpert ion gauge (Varian UHV-24 / Leybold Ionivac IM520 was used.

The upper level seen in Figure 2.2 is equipped with a quartz micro balance (QMB), a zinc evaporator (ZE), a sputter gun (SG), a quadrupol-mass-spectrometer (Pfeifer QMS 200; QMS) and an infrared source (Brucker 66 v/S FTIR; IRS) with external detector (IRD). Additionally the optical path of the infrared beam (marked red) is shown.

The lower level seen in Figure 2.3 is equipped with a hemispherical mirror analyser (HMA) and an x-ray source (XA) to perform XPS spectroscopy. Furthermore there is low energy electron diffraction (Specs ErLEED 150; LEED) and two ionisation gauges (IG) as well as three leak valves for oxygen, argon and methanol in the lower level.

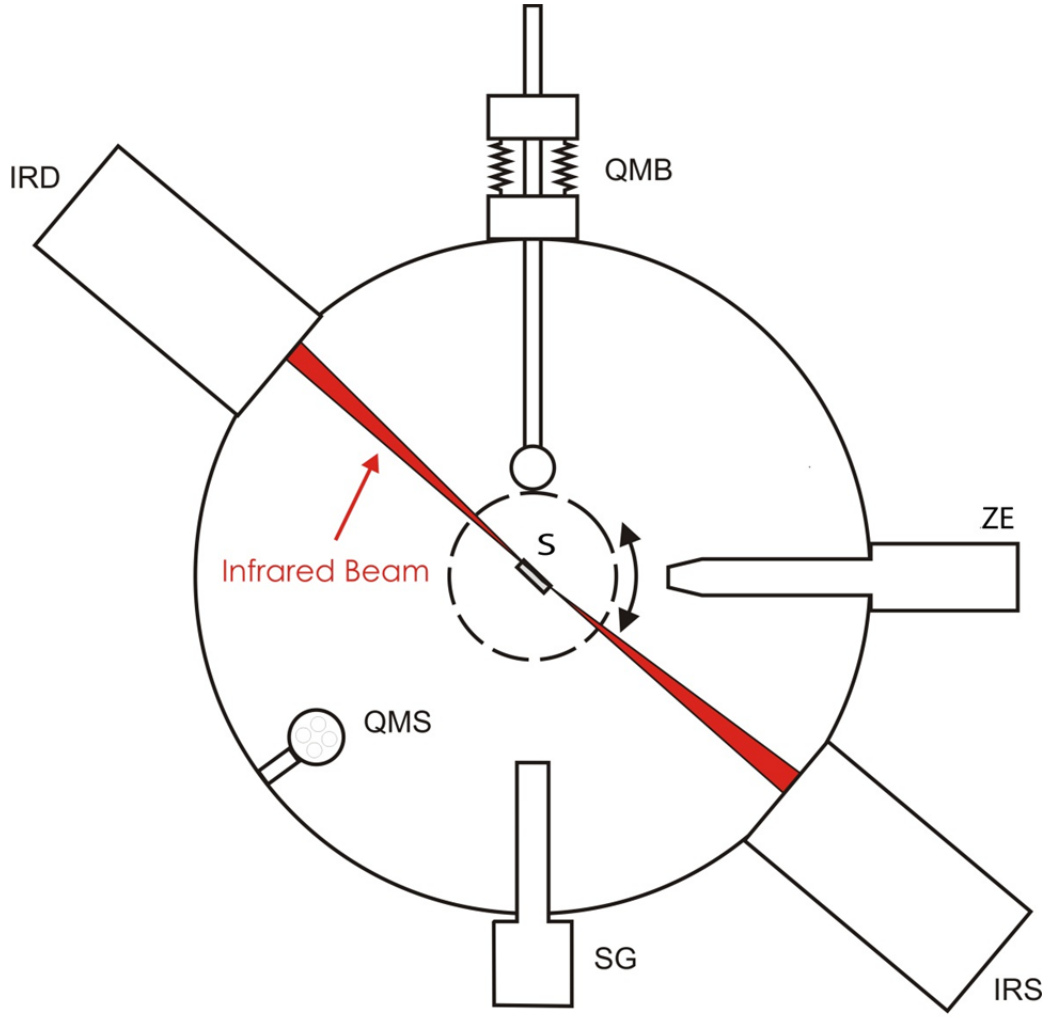

Figure 2.2: UHV chamber upper level; adapted form [7].

IRD – Infrared detector
QMB – Quartz microbalance
ZE – Zinc evaporator
IRS – Infrared source
SG – Sputter gun
QMS – Quadrupol mass spectrometer
S – Sample

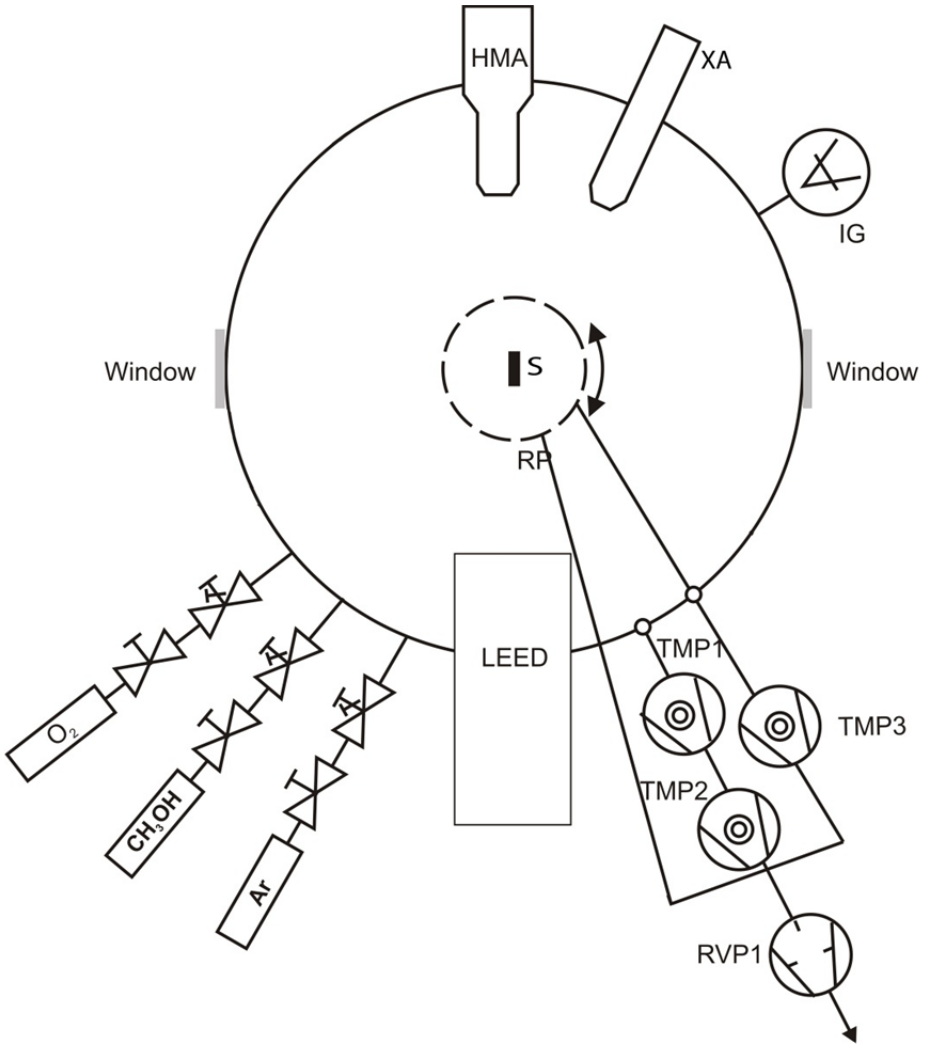

Figure 2.3: UHV chamber lower level; adapted form [7].

HMA – Hemispherical mirror analyser
XA – X-ray anode
IG – Ionisation gauge
LEED – Low energy electron diffraction
Ar – Argon valve
CH_3OH – Methanol valve
O_2 – Oxygen valve
RP – Rotary platform
S – Sample
TMP1 – Turbo molecular pump 1
TMP2 – Turbo molecular pump 2
TMP3 – Turbo molecular pump 3
RVP1 – Rotary vane pump 1

2.2. The sample and sample mounting

2.2.1. Current setup

The sample which is used in the following series of experiments is a Pd (111) single-crystal. It is disk shaped with a diameter of 10 mm and provided with a groove which is milled into its rim. Two tantalum (Ta) wires (0.25 mm) are routed through the rim holding the crystal in place (Figure 2.4). The wires ends were tightened between electrical contacts which are fixed to the main holder with ceramic insulators in between. This assembly allows resistive heating to approximately 1120 K. To get best thermal conduction the sample mount is made of copper and attached to a tube that can be filled with liquid nitrogen.

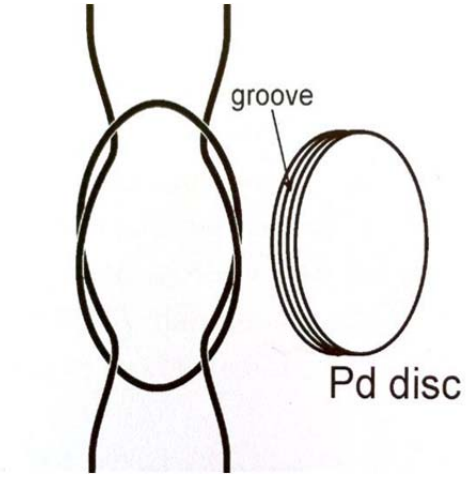

Figure 2.4: Pd crystal mounted with tantalum wires; adapted form [8].

On the backside of the crystal a thermocouple is spot welded to monitor the sample temperature (Figure 2.5).

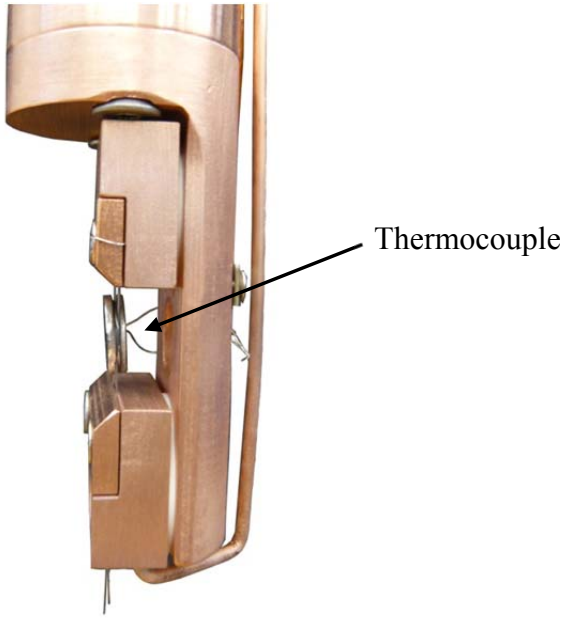

Figure 2.5: Sample holder

2.2.2. **Changes to the previous setup**

Due to the fact that cooling limitations occurred during the master thesis of F. Weber [7], the sample mounting was redesigned[2]. Its width was almost doubled. A comparison is shown in Figure 2.6. The use of additional copper allowed sample cooling to 123 K during experiments, while F. Weber was limited to 173 K. Additionally, the cooling rate was increased drastically. Another change of design is seen in Figure 2.7. The wires of the thermocouple element are now fed through a hole in the back of the sample holder (Figure 2.7 (b)). In the old design cables had to be fixed to the side of the holder after mounting (Figure 2.7 (a)).

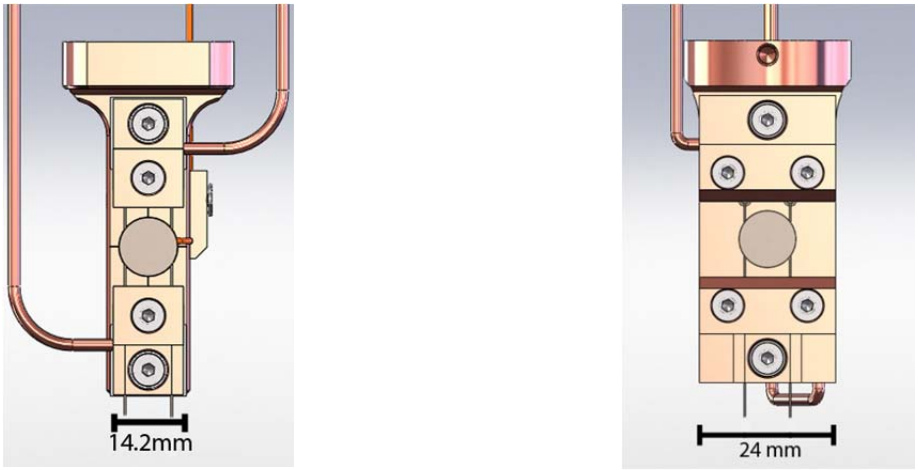

(a) (b)

Figure 2.6: Gain in width; old (a) vs. new (b) sample holder; frontal[3]

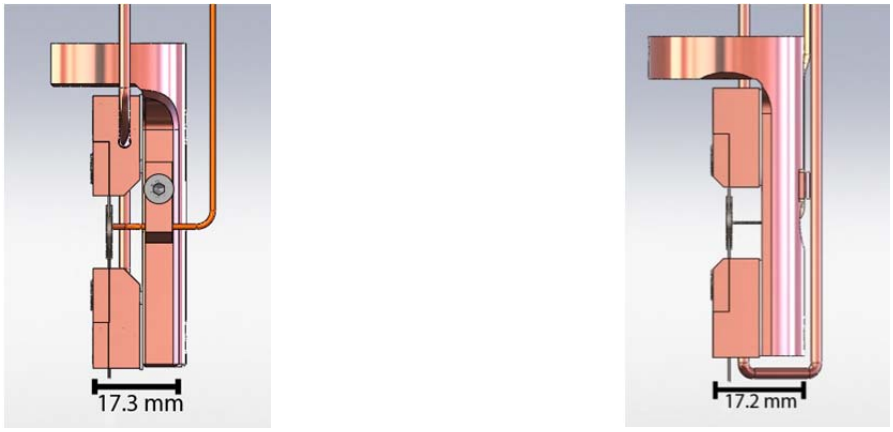

(a) (b)

Figure 2.7: New feed through; old (a) vs. new (b) sample holder; lateral view[4]

[2] by R. Schennach and M. Kornschober
[3] Figures made by M. Kornschober
[4] Figures made by M. Kornschober

2.3. Equipment

2.3.1. Fourier Transform Infrared Spectroscopy (FTIR)

Infrared spectroscopy is a physical analysis method to obtain an infrared spectrum of absorption and/or emission of a solid, liquid or gas using infrared light. It was used to investigate absorbed species on the sample surface and allowed direct statements about the presence and concentration of infrared-active functional groups.
A reflection absorption infrared spectroscopy (RAIRS) setup was used in the experiments. Below a short overview is given (for further information see [[9], [7], [10]]).

Infrared spectroscopy was done with a Brucker IFS 66 v/S FT-IR spectrometer. The emitted infrared beam is send through the UHV camber where it is reflected by the sample to the external detector. A schematic is shown in Figure 2.8. The detector is made out of mercury-cadmium-telluride (MCT) which allows faster detection and higher sensitivity than its competitors [11]. To reduce noise the detector has to be cooled with liquid nitrogen.

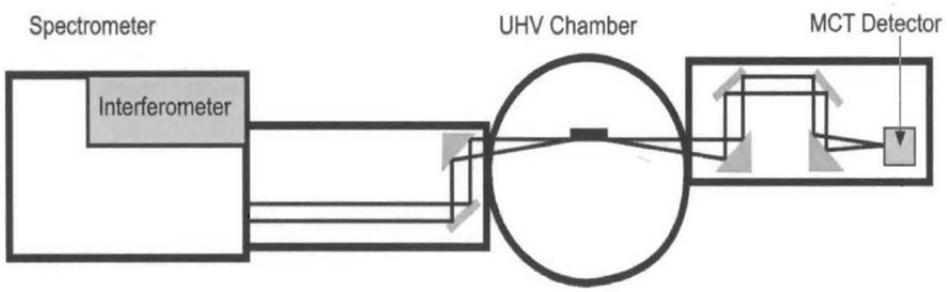

Figure 2.8: Schematic of RAIRS setup; adapted from [10].

A SiC Globar was used as an IR light source. The emitted light is sent in the Michelson interferometer, a schematic is seen in Figure 2.9. It is able to modify the beam to contain different combinations of frequencies. The interferometer consists of a beam splitter (Ge/KBr) and two mirrors. One mirror is fixed and the other one moveable and nitrogen gas cushioned. When the IR-beam has passed through the Michelson interferometer it is send towards the sample surface in a very flat angle.

At the sample surface the electromagnetic wave can interact and energy changes can occur. If energy is absorbed by atoms or molecules they can go from their ground state to an excited state. The energy difference between these two states, is equivalent to the energy of the absorbed radiation (photons) and is closely related to the structure of atoms or molecules.

This is done many times with different combinations of frequencies. Then a computer calculates (Fourier transformation) the absorption at each wavelength, generating the whole spectra.

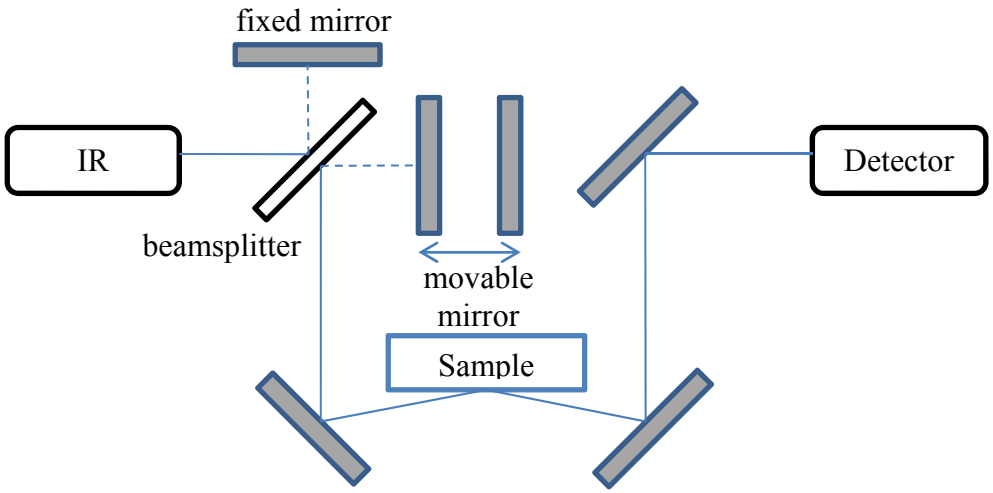

Figure 2.9: Schematic view of a Michelson interferometer

To reduce the strong water and carbon dioxide bands as a result of air, the whole optical path is evacuated to a pressure below 2 mbar. Additionally, the detector is equipped with a cold trap, filled with liquid nitrogen, to further reduce the interference caused by water in air.

To get an IR-spectrum, an interferogram is measured and then transformed into a single channel signal using Fourier transformation. In Figure 2.10 (a) two single channel spectra are seen. The black curve shows a Pd/ZnO surface whereas the red curve shows a Pd/ZnO surface with methanol. To obtain a transmission spectrum the single channel signal (ΔR / red line) has to be divided by a single channel signal reference spectrum (R° / black line) from a reference sample surface. Transmission T, seen in Figure 2.10 (b), is the result of dividing the change of reflectance ΔR by the initial value of the reflectance $R°$(2.1).

$$T = \frac{\Delta R}{R°} \qquad \textbf{(2.1)}$$

To prevent temperature shifts it is of great importance to measure the reference spectrum and the actual spectrum at the same temperature.

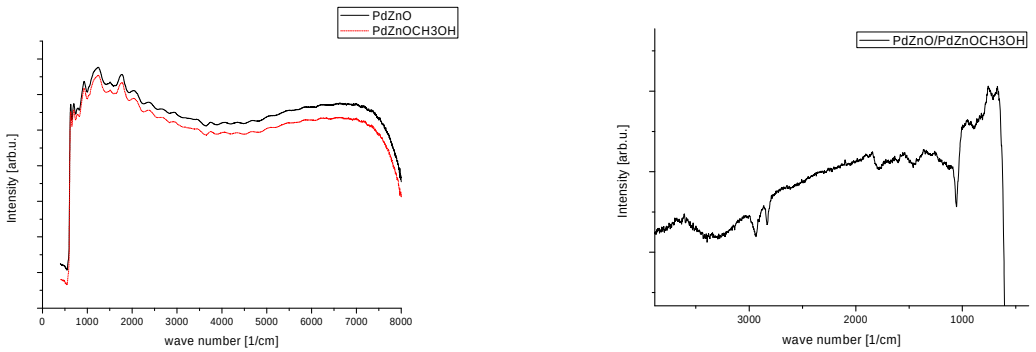

(a) (b)

Figure 2.10: How to obtain FTIR spectra; (a) Single channel signal, (b) Transmission spectrum

2.3.2. **X-ray Photoelectron Spectroscopy (XPS)**

X-ray photoelectron spectroscopy was used to ensure a clean sample surface. It was also used to observe chemical composition of the Zn and ZnO films on the sample surface. It is a very surface sensitive method because only emitted photoelectrons near the surface escape and are measured. This is due to the fact that the mean free path of photoelectrons in a solid is only a few micrometers long. Below a short overview is given (for further information see [12]).
The XPS-system consists of four main parts. In Figure 2.11 the x-ray source (a), the sample (b), the retarding lens system (c), the electron analyzer (d) and the detector (e) is shown.

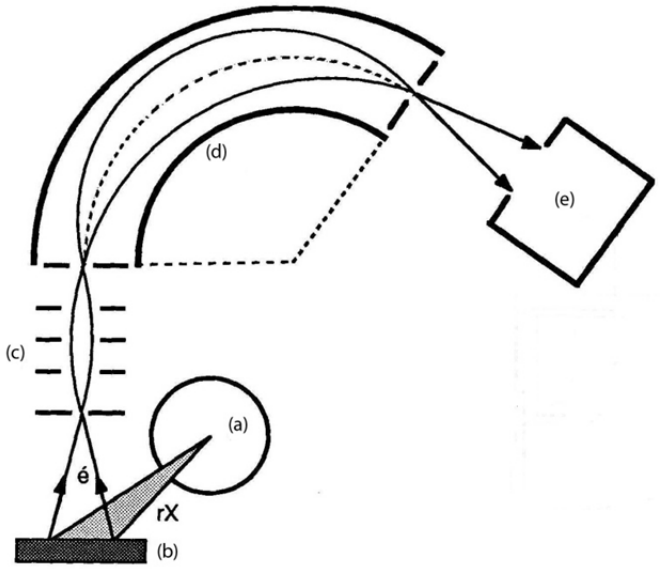

Figure 2.11: Schematic view of a XPS-system; adapted form [13].

The X-ray photoelectrons are obtained by using an x-ray tube. It is equipped with switch able magnesium and aluminum anodes providing characteristic radiation on a bremsstrahlung background (Al-K_α 1486,6 eV / Mg-K_α 1253,6 eV). In all experiments the Mg-anode was used. The obtained photoelectrons are sent towards the sample surface. There bound electrons are knocked out and escape the sample surface heading towards the analyzer. These electrons have kinetic energies given by

$$KE = h\upsilon - BE - \phi_s \quad \textbf{(2.2)}$$

Where $h\upsilon$ is the energy of a photon, BE is the binding energy of the atomic orbital from which the electron originates, ϕ_s is the work function of the spectrometer and KE is the kinetic energy of an electron.
The analyzer is a concentric hemispherical analyzer with an additional retarding lens system for resolution improvement. It separates electrons with different energies. At the end of the analyzer an electron multiplier (channeltron) was used to detect incoming electrons.

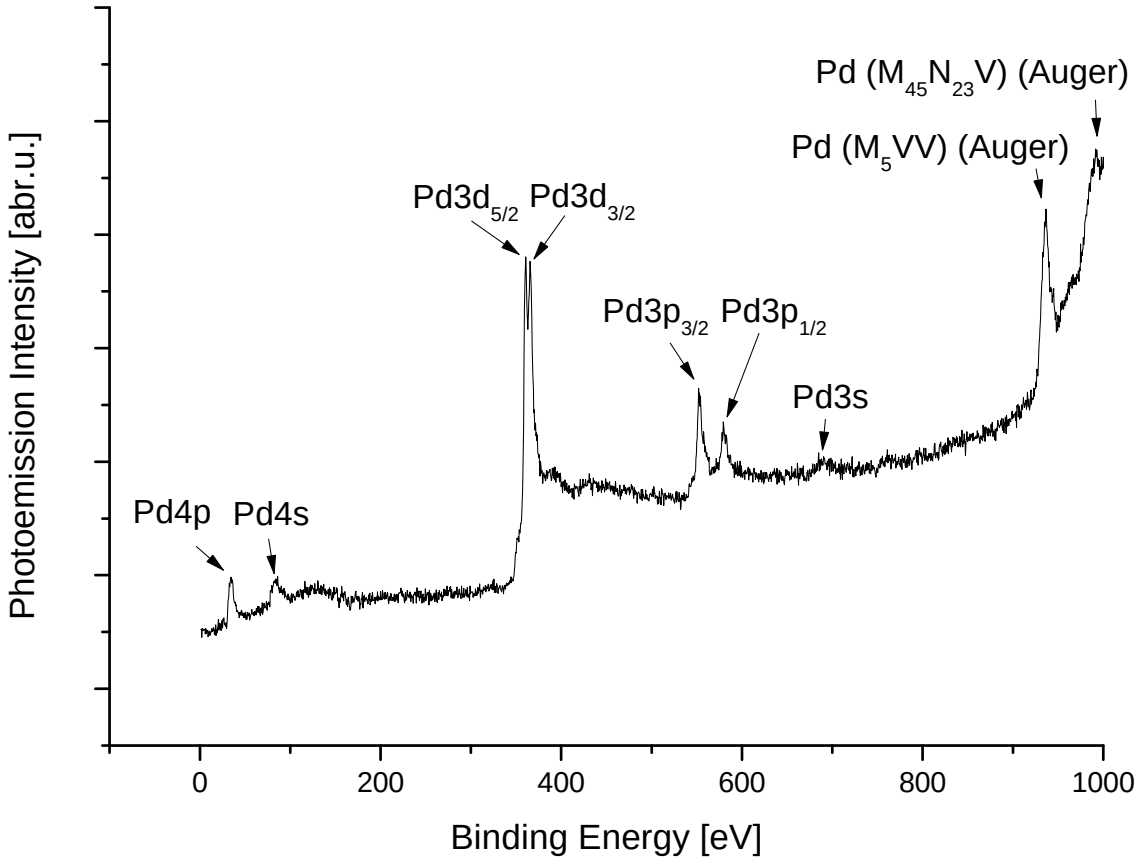

Figure 2.12: XPS spectra of the clean Pd sample

In Figure 2.12 a spectrum of the clean Pd sample is shown. Only characteristic Pd peaks (Pd4p, Pd4s, $Pd3d_{5/2}$, $Pd3d_{3/2}$, $Pd3p_{3/2}$, $Pd3p_{1/2}$, Pd3s, $Pd(M_5VV)$, $Pd(M_{45}N_{23}V)$) are seen.
For example, $Pd3p_{1/2}$ means that the electrons originate from a 3p orbital of a Pd atom where the denotation provides information about the total angular momentum of an electron.
.

2.3.3. **Low Energy Electron Diffraction (LEED)**

The low energy electron diffraction apparatus is used to observe the surface structure of thin films and clean or adsorbate covered crystal surfaces. Below a short overview is given (for further information see [14], [15]).

The low energy electron diffraction apparatus consists of two main parts: an electron gun and a detection system. The electron gun produces a well collimated and monoenergetic electron beam pointed at the sample. The electron energy can be varied between 0 to 1000 eV. If beam electrons hit the sample surface they get back-scattered through grids towards the detector.

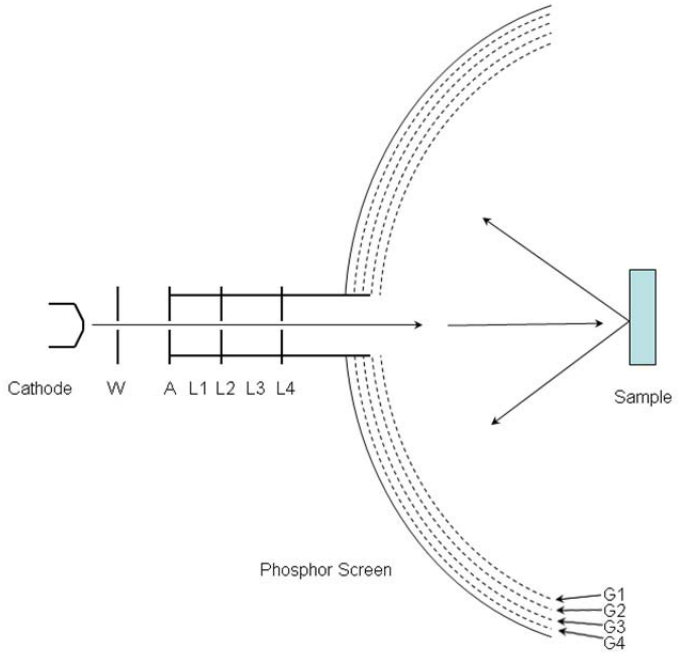

Figure 2.13: Schematic view of a LEED display-system; adapted form [16].

In Figure 2.13 the LEED system is shown in detail. The electron gun consist of a cathode, a Wehnelt cylinder (W), a double anode (A) and 4 lens elements (L1,L2 L3,L4). The detector is a concentric fluorescent screen. Four grids, which are made out of gold coated molybdenum are placed in front of it. The first grid (G1) is grounded so that scattered electrons from the sample are not deflected. The second grid (G2) is at a negative potential. It is slightly smaller than the primary electron energy which allows only the elastically scattered electrons to pass. The inelastically scattered electrons get deflected. The third grid (G3) is at the same potential as the second. Its use is to reduce field inhomogeneities. The fourth grid (G4) is on earth potential. Electrons that pass all four grids are accelerated towards the florescent screen because of its positive potential of a few kilovolts. If an electron hits the screen it creates a light spot. A diffraction pattern in the form of the reciprocal lattice of the sample can be observed. [15]

2.3.4. **Quadrupol Mass Spectrometer (QMS)**

A quadrupol mass spectrometer (Pfeiffer QMS 200) was used to analyze the residual gas. Below a short overview is given (for further information see [17]).

A QMS consists of three main parts: the ion source, the analyzer and the detector (Figure 2.14).

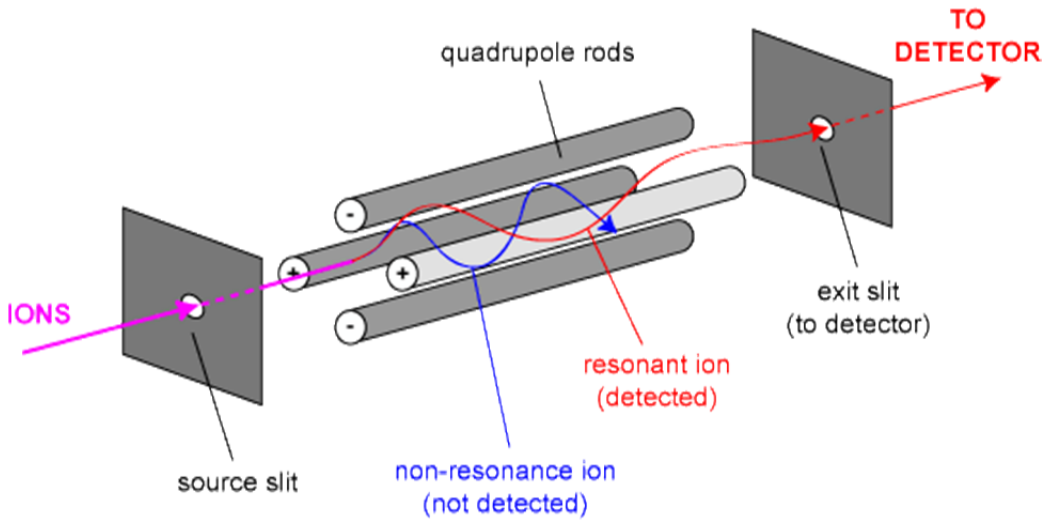

Figure 2.14: Schematic view of a quadrupol mass spectrometer; adapted form [18].

Uncharged atoms of the residual gas are ionized by electron bombardment (ion source). Now the ions enter the quadrupol field which is created by four parallel mounted metal rods (electrodes). Within this structure counterpart rods have the same polarity. As the geometry of the rods is given, depending on the applied potential, only particles with a particular energy to mass ratio can reach the end of the analyzer. At the end of the analyzer a secondary electron multiplier (SEM) is amplifying the signal of incoming particles [17].

Ion source

In an ion source electrons are accelerated from an anode to a cathode and send through the gas under investigation. If a highly energetic electron collides with a gas molecule a second electron gets "knocked out" of its hull which induces ionization. The result is a positive charged ion with the same mass as the original molecule. A second possibility is that, due to the very high energy of the electrons gas molecules get fragmentized. Reducing the energy of the electrons would lead to less fragmentation but also to a decrease of ion yield. Finally the Ions are directed towards the separation system [19].

Separation system

The separation system consists of four metal rods (electrodes), where overlapping AC and DC voltages are applied, and as a consequence create an electrical field ϕ (2.3). This field separates the ions according to their mass/energy ratio.

$$\phi = U + V \cdot \cos(\omega t)\frac{x^2 - y^2}{r_0^2} \qquad \textbf{(2.3)}$$

Where x and y are the distances along the given coordinate axes, r_0^2 is the distance from the centre axis (the z axis) to the surface of any electrode, ω is the angular frequency ($2\pi f$) of

the applied ac waveform, V is the magnitude of the applied ac or RF waveform, and U is the magnitude of the applied dc potential.
The equations of motion for each axis are given in equations (2.4), (2.5) and (2.6), which lead to Mathieu's differential equations. In particular it can be proven that solutions of differential equations of this type can be either bounded or unbounded solutions. Physically, a bounded solution corresponds to a case where the ion travels through a field without changing direction. An unbound condition however means that the ion will crash on one of the electrodes and as a result does not reach the detector [19].

$$F_x = -[U + V \cdot \cos(\omega t)]\frac{ex}{r_0^2} \quad \textbf{(2.4)}$$

$$F_y = [U + V \cdot \cos(\omega t)]\frac{ey}{r_0^2} \quad \textbf{(2.5)}$$

$$F_z = 0 \quad \textbf{(2.6)}$$

Detector

If ions reach the end of the analyzer they get into the detector. First the signal of an incoming ion is amplified to make detection easier. This is done by a channeltron. It is made out of a small glass tube. The inner walls of the tube are coated with a high resisting film. One end is the ion inlet which is open the other end is the detector anode which is closed. An incoming ion produces an electron cascade towards the anode which can be easily detected [19].

2.3.5. **Bayard-Alpert ionization gauge**

The Bayard-Alpert ionisation gauge was used to measure the total pressure in the vacuum chamber. Its operation area is from 10^{-1} to 10^{-10} mbar. Below a short overview is given (for further information see [20]).

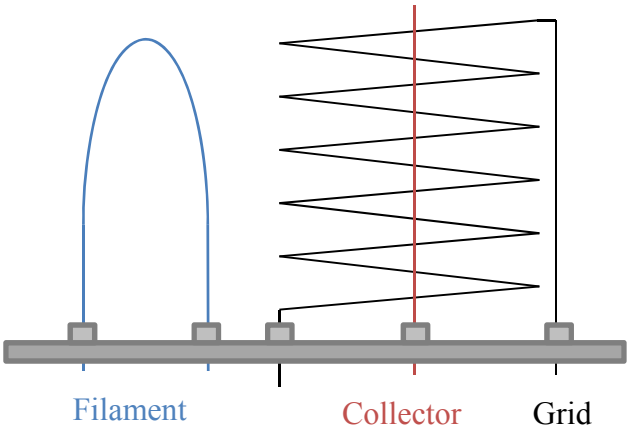

Figure 2.15: Schematic view of a Bayard-Alpert ionisation gauge

In Figure 2.15 a schematic of a Bayard-Alpert Ionisation gauge is seen. It consists of a filament (anode), a grid and a collector (cathode). Its working principle is simple. Electrons emitted by the filament pass through the grid several times where they ionise residual gas molecules which travel to the collector resulting in a current between anode and cathode. Since the number of ions produced per electron is proportional to the gas density, the measured current is an indicator for the pressure in the chamber. But the ionization probability differs from gas species to gas species. For this reason it is necessary to calibrate the manometer before use for one single gas. Usually nitrogen is used for this purpose. This is the reason why gases with different ionization energy than nitrogen are not taken to account equally. As a result a Bayard-Alpert ionization gauge is only able to measure the relative total pressure [19].

2.3.6. **Sputter gun**

The sputter gun (Perkin Elmer PHI Model 04-161 Sputter Ion Gun) was used to clean the sample surface. Below a short overview is given.

The sputter gun accelerates argon ions towards the sample surface which sputter out the contaminants. In this process the surface structure is damaged because not only surface contaminants but also sample surface layers are removed during the bombardment.
To create an Argon pressure ($5*10^{-5}$ mbar) in the vacuum chamber a dosing valve is opened. The Argon ions are accelerated from the sputter gun (anode: 1.5kV/25mA) to the sample surface (cathode). In experiments done in this thesis sputter times between 30 and 60 minutes proved to clean the sample surface effectively. Short sputter times may not remove all contaminants from the surface where too long sputter times may release contaminants long buried under the sample surface. After this process the sample has to be heated to 1120 K. Heating up the sample allows the crystal to reconstruct to its initial state and return to a plain sample surface [19].

2.3.7. **Thermal Desorption Spectroscopy (TDS)**

In this master thesis thermal desorption spectroscopy (TDS) was used to investigate the decomposition products of methanol from Pd, Pd/Zn and Pd/ZnO. It is a very important method to study reactants of a catalytic reaction desorbing from a solid. Below a short overview is given (for further information see [21], [22], [23]).

In theory, the desorption process can be described by the Polanyi-Wigner-equation:

$$r_d = -\frac{d\theta}{dt} = \nu_n(\theta)\cdot\theta^n \exp\left(-\frac{E_d(\theta)}{RT}\right) \qquad \textbf{(2.7)}$$

r_d	Rate of desorption
t	Time
n	Kinetic order of the desorption process
E_d	Desorption energy
θ	Coverage
R	Gas constant
υ_n	Preexponential factor
T	Temperature

The peak shape of the desorption signal allows conclusions on the order of desorption.

First-order desorption kinetics (n=1) show an asymmetric TDS-signal. The temperature at which the maximum rate of desorption occurs is invariant with the surface coverage (Figure 2.16 (A)). It indicates a single surface species which is molecularly bonded.

On the other hand, second-order desorption kinetics (n=2) show a symmetric TDS-signal. The temperature at which the maximum rate of desorption occurs shifts to lower values as the surface coverage increases (Figure 2.16(B)). It indicates the associative desorption.

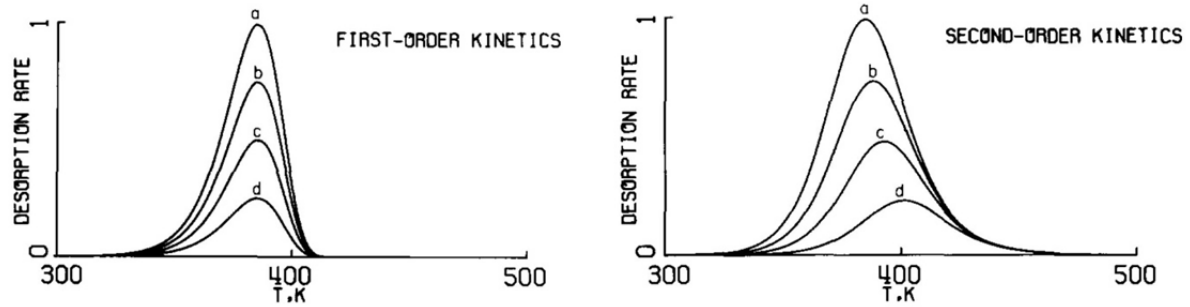

(A) (B)

Figure 2.16: Illustration of desorption spectra: (A) first-order desorption, (B) second-order desorption; adapted form [22].

TDS-spectra were also used to calculate the Zn-coverage of the sample. For further information see chapter 2.4.

2.3.8. **Zn evaporator**

The zinc evaporator was used to deposit thin Zn or Zn/O films on the sample. Below a short overview is given (for further information see [8]).

For Zinc deposition a custom made evaporator was used[5]. It consists of two main parts, an evaporator (Knudsen cell) and a shutter (marked red in Figure 2.17).

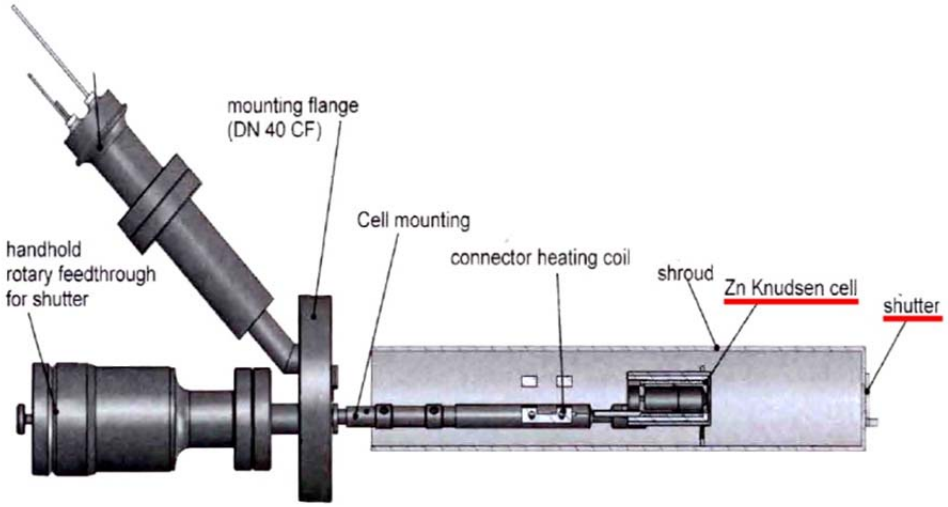

Figure 2.17: Zn evaporator; adapted form [8].

The evaporator is a simple Knudsen cell. Two interleaved molybdenum cylinders were filled with Zn (GOODFELLOW, lump size max. 2 mm; purity: 99,98 %). On one side the cylinder was equipped with a hole for the Zn outlet and on the other side with a Ni/CrNi-thermocouple. The molybdenum cell is surrounded by a resistive heating system. The whole construction is mounted in a stainless steel tube. Figure 2.18 shows a cross section of the Knudsen cell.

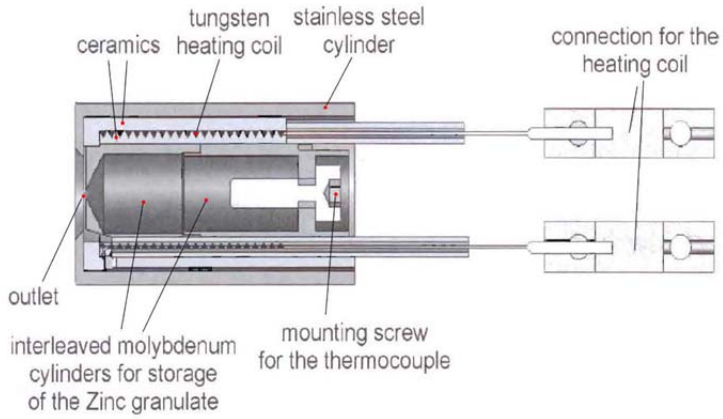

Figure 2.18: Cross section of the Zn Knudsen cell; adapted form [8].

The shutter is placed in front of the outlet (Ø 8 mm) to ensure exact deposition times.

[5] Designed by M. Kornschober during the PhD thesis of M. Kratzer [8].

2.4. Production of Zn and ZnO monolayers on Pd (111)

2.4.1. Cleaning

The Pd crystal surface is cleaned by a sputter gun (anode: 1.5kV/25mA) in an Ar atmosphere ($5*10^{-5}$ mbar). Sample cleaning position was x=4, y=4,6, z=23 and θ=42°. The crystal temperature is kept at 432 K during the process. After 60 minutes of sputtering the Ar valve is closed and the annealing process is started by heating up the sample to 1123 K. This temperature is maintained for four minutes. After the third minute the O valve is opened until a pressure of $8.5*10^{-8}$ mbar is reached. Then the heating is turned off and the sample is cooled down. At room temperature (300 K) the O valve is closed and a second annealing process is started. This time the sample is heated up to 1123 K and cooled down without oxygen in the UHV chamber. After this cleaning process the sample surface was analyzed with XPS. An XPS spectrum from a clean sample surface is shown in Figure 2.12 on page 12.

2.4.2. Production of a Zn monolayer

After the cleaning process the sample temperature is kept at 300 K and is positioned to face the Zn evaporator shutter (x=4, y=4, z=23, θ=135°). The temperature of Zn is kept stable at 595 K to obtain a constant evaporisation rate. Then the shutter was opened for a specific amount of time. After that the sample is positioned to face the QMS (x=3.3, y=3.3, z=23, θ=0°) and heated up to 1123 K while the QMS is detecting the mass 64 over time.

In Figure 2.19 three thermal desorption spectra of mass 64 (Zn) for different exposition times are seen. If Zn exposition time is reduced, the multilayer peak at about 500 K is decreasing until it disappears completely. This is traced back to the fact that the bond between Zn atoms is weaker than the bond between Zn and Pd [[24], [25], [26]]. So the multilayer of Zn desorbs at low temperature while the monolayer desorbs at high temperature.

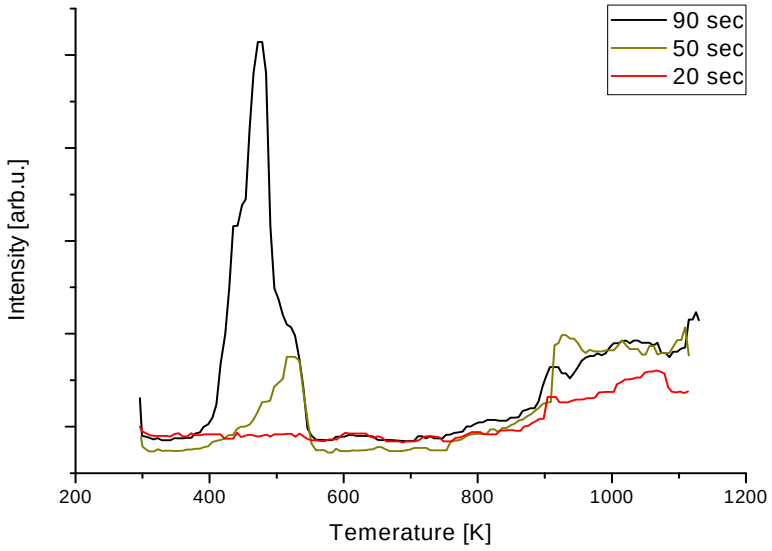

Figure 2.19: Decreasing multilayer peak as a function of Zn exposition time

As a consequence, a spectrum which does not show a low temperature peak is considered to show a monolayer of Zn.
For calibration a spectrum where the low temperature peak is just not shown any more is used. In Figure 2.20 the spectra of mass 64 as a result of 20 second Zn coverage is shown in detail. More than 20 seconds of Zn exposition would lead to a low temperature peak (->

multilayer), less than 20 seconds would lead to a sub monolayer. The fact of a missing low temperature peak leads to the assumption that a monolayer was applied [[24], [25]]. The area beneath the curve is proportional to the amount of desorbed Zn from the sample surface.
It was necessary to extend the curve with a Lorenz fit to be able to calculate the area beneath the peak. The area was calculated to $3.96246*10^{-10}$.

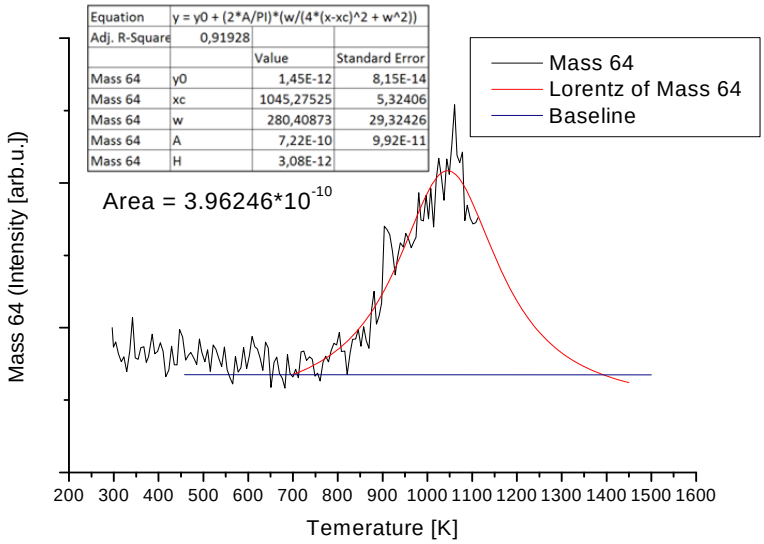

Figure 2.20: TDS used to calculate Zn coverage

In the absence of any segregation, Zn films on a Pd (111) single crystal are homogeneous with the same stoichiometry for each layer [4]. Knowing the amount of Pd atoms on the sample surface gives direct information about the number of Zn atoms necessary to build a monolayer on it.
The (111) bulk-terminated Pd surface has $1.53*10^{19}$ Pd surface atoms/m^2 [5]. The sample surface (front) has ~78.53 mm^2. Doing some calculation[6], the sample surface has approximately $1.01*10^{15}$ Pd atoms. Therefore the calculated area beneath the peak (shown in Figure 2.20) is the result of ~$1.01*10^{15}$ desorbed Zn atoms.

2.4.3. **Production of a ZnO monolayer**

After a cleaning process the sample temperature is kept at 300 K and it is positioned to face the Zn evaporator shutter (x=4, y=4, z=23, θ=135°). The O valve is opened to create an O atmosphere. Then the Zn shutter is opened for a particular amount of time and closed again. After the Zn exposure the Pd crystal is heated up to 550 K and cooled back down to 300 K. When 300 K are reached the oxygen valve is closed.

Depending on the oxygen pressure provided during Zn exposure different ZnO structures can be found. In Figure 2.21 STM and LEED pictures of the possible ZnO structures are shown.
Figure 2.21 (A) shows a STM picture of a (4 x 4) structure where the parallelogram marks the unit cell of the Pd structure. The inside of the seen hexagons consists of three Zn atoms.
Figure 2.21 (B) shows the corresponding LEED picture of a (4 x 4) structure characterized by three ZnO spots between two Pd spots. They are hardly seen because the structure is very fast destroyed by the electron beam.

[6] See Appendix

Figure 2.21 (C) shows a STM picture of a (6 x 6) structure where the small parallelogram again marks the unit cell. The large parallelogram shows the (6 x 6) superstructure.
Figure 2.21 (D) shows the corresponding LEED picture of a (6 x 6) structure characterized by six hexagonal arranged spots representing Pd. Between two Pd spots five ZnO spots can be found [26].

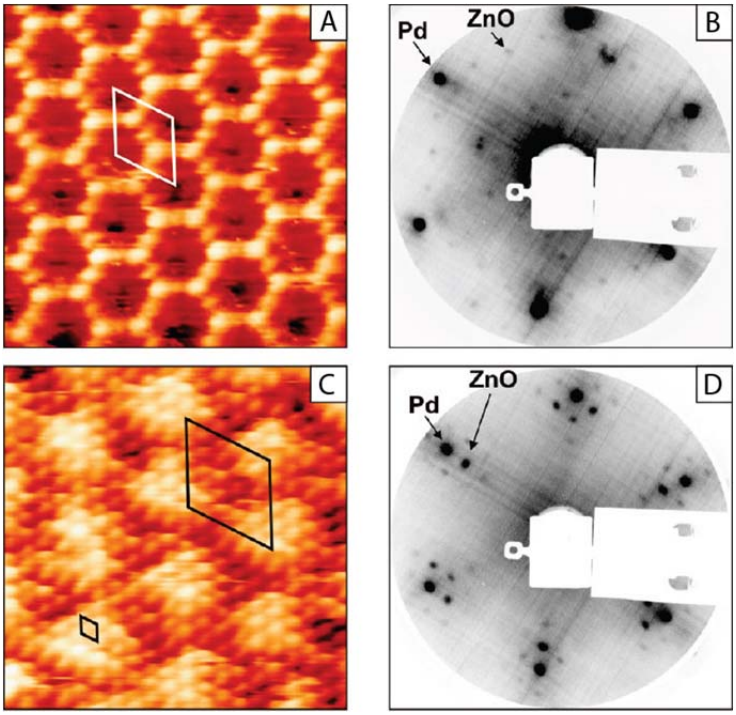

Figure 2.21: (A) STM image (65 Å x 65 Å) of a (4 x 4) structure ZnO; (B) LEED image of a (4 x 4) structure ZnO; (C) STM image (50 Å x 50 Å) of a (6 x 6) structure ZnO; (D) LEED image of a (6 x 6) structure ZnO; adapted from [26]

Low oxygen pressure of $5*10^{-8}$ mbar results in a Pd(111) surface covered by (4 x 4) and (6 x 6) structured ZnO islands (Figure 2.22 A). Increasing the pressure to $1*10^{-7}$ leads to changes in ratio between (4 x 4) and (6 x 6) structured ZnO islands. The area covered by (6 x 6) islands decreases with respect to area covered by (4 x 4) islands (Figure 2.22 B). The structure changes dramatically when oxygen pressure reaches $1*10^{-6}$ mbar. The single layer (6 x 6) islands become replaced by smaller but higher islands. The (4 x 4) islands remain unaffected. Figure 2.22 C (inset) shows the line profile (along the black line) of the sample surface. A clear change in island height can be seen. An oxygen pressure above $5*10^{-6}$ mbar results in full conversion, also of the (4 x 4) islands, to bilayer islands (Figure 2.22 D) [26].

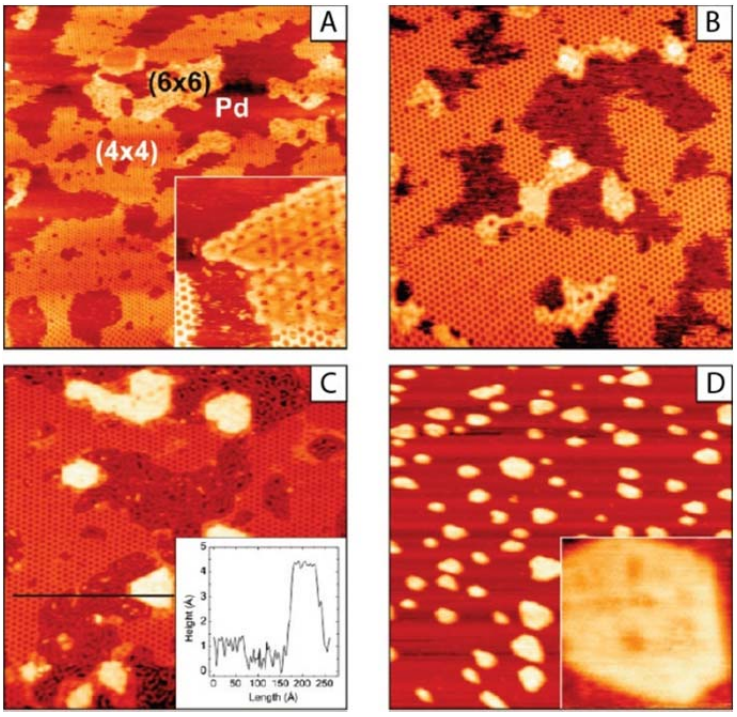

Figure 2.22: STM images of sub monolayer ZnO coverages prepared under different oxygen pressures: (A) $5*10^{-8}$ mbar; (B) $1*10^{-7}$ mbar; (C) $1*10^{-6}$ mbar [inset: line profile taken along the line (black), indicated on the image]; (D) $5*10^{-6}$ mbar; adapted from [26]

To produce a monolayer of ZnO on the sample surface it is necessary to know how much Zn exposure creates a monolayer of Zn. This is important because ZnO on Pd is not showing any low temperature multilayer peaks in TDS for calibration. It is known that one single layer of ZnO corresponds to a surface coverage of Zn atoms of ~0.7 [22]. The desorption curve of mass 64 from ZnO is compared to the desorption curve of mass 64 from a Pd/Zn (monolayer) surface. Therefore ~$3.363*10^{15}$ Zn atoms are necessary to create a ZnO monolayer on Pd(111).

3. TDS – Study of methanol desorption from Pd (111), Pd/Zn and Pd/ZnO

Several methanol desorption experiments from Pd(111), Pd/Zn and Pd/ZnO where done to investigate their catalytic effect. An overview of TDS-measurements is given in chapter 2.3.7 and in more detail in [[21], [22], [23]].

TDS experiments were always performed in the exact same way to ensure comparability. The following description shows the measurement process.

1. Cleaning: The sample surface was cleaned and annealed (see chapter 2.4.1).

2. Zn/ZnO layer: Depending on the experiment, a Zn or ZnO layer was created on the sample surface (see chapter 2.4.2).

3. Cooling: The sample was cooled down to 123 K.

4. Methanol exposition: depending on the experiment the methanol valve was opened. To investigate a variety of methanol film thicknesses the methanol pressure and exposition times were altered.

5. TDS: The sample was heated to 1123 K (heating rate 1K/s). During the heating process the QMS measured the intensity of reactants (see Table 3.1) desorbing from the sample surface (see chapter 2.3.7).

Mass	***Formula***	***Compound***
2	H_2	Hydrogen
18	H_2O	Water/Methanol fragment
28	CO	Carbon monoxide/Methanol fragment
29	CH_2O	Formaldehyde/Methanol fragment
31	CH_3O	Methanol fragment
32	O_2	Oxygen/Methanol
44	CO_2	Carbon dioxide
45	CO_2H	Formate
64	Zn	Zinc

Table 3.1: Detected Mass and corresponding species

3.1. Methanol desorption from Pd/Zn and Pd/ZnO

3.1.1. First series of experiments: Pd/Zn

The first series of measurements was dedicated to methanol desorption from Pd/Zn. The aim was the investigation of sub monolayers of Zn on Pd. Two experiments were done.
A desorption spectrum of hydrogen is shown in Figure 3.2. Original data as well as smoothed data is plotted. Data smoothening has been applied to all spectra because of the rather high signal to noise ratio.

1. 0.4 ML Zn were deposited on the sample surface at room temperature. Then the sample was cooled down to 123 K for methanol exposition. A dosage of 0.38 L methanol was given. Figure 3.3 shows the thermal desorption spectra of methanol form Pd/Zn (red line).

2. 0.2 ML Zn were deposited on the sample surface at room temperature. Then the sample was cooled down to 123 K for methanol exposition. A dosage of 0.75 L methanol was given. Figure 3.3 shows the thermal desorption spectra of methanol form Pd/Zn (black line).

The resulting sample surface before methanol exposition is shown in Figure 3.1. Sub monolayer Zn films form 2D islands (white) on the Pd sample surface (black). The inset shows the corresponding LEED image where the weak (2 x 2) pattern is seen [25].

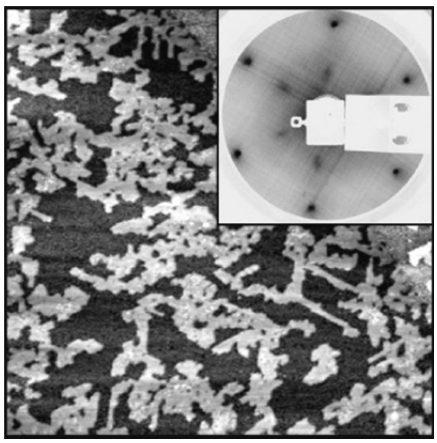

Figure 3.1: STM image (1000 Å x 1000 Å) of 0.5 ML Zn on Pd (111) with corresponding LEED image [inset]; adapted from [25]

In Figure 3.2 a major peak is seen from 240 K to 416 K. A second peak starts at 840 K (red marked area). This peak, shown in every measured mass, is a result of desorption from the sample holder.
A slight rise in temperature of the sample holder during the heating process of the sample was observed with an additional thermo couple element. Further increase in the temperature of the parts, where the tantalum wires were mounted, could not have been avoided. Therefore, the peak shown after 840 K is of no relevance. Consequently, all following spectra are shown until 850 K. With the one exception of zinc (mass 64), which shows a high temperature peak beyond 850 K.

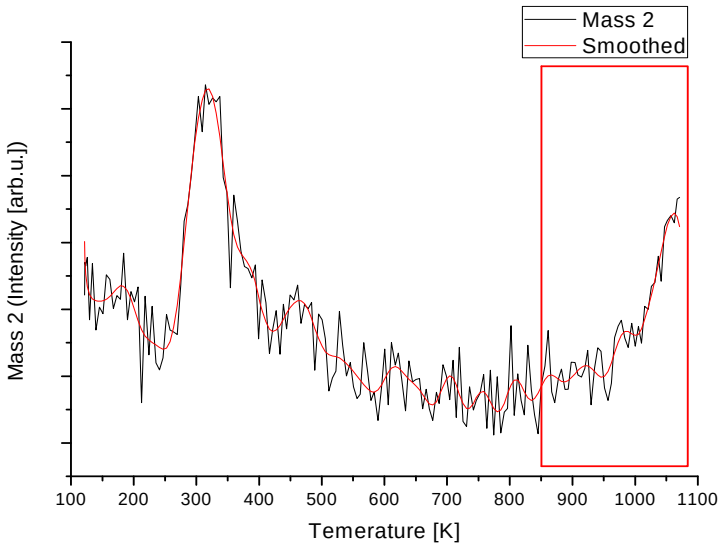

Figure 3.2: Visualisation of original data compared to smoothed data

In Figure 3.3 (a) the desorption spectra of hydrogen (mass 2) is shown. Both experiments show hydrogen desorption at ~324 K.

In Figure 3.3 (b/c/d/e/f) the desorption spectra of water/methanol, carbon monoxide, formaldehyde/methanol, methanol and oxygen/methanol (mass 18/28/29/31/32) are shown. They all display the same curve shape for each experiment. In experiment one there are two peaks at the exact same temperature. The first peak at 178 K and the second one at 461 K. Experiment two shows almost no desorption at all, due to the fact that only half the methanol dosage was given.

In Figure 3.3 (g/h) the desorption spectra of carbon dioxide and formate is shown. As can be seen almost no carbon dioxide and formate desorption were measured in both experiments.

Figure 3.3 (i) shows the desorption spectrum of zinc. Both experiments show nearly the same results, Zinc desorption starts at 903 K which is almost where it is expected to be [5] considering the temperature-measurement-error[7]. Trying to prevent damage from the tantalum wires, the maximum heating current was limited. As a result it was not possible to reach the end of the peak.

[7] See Appendix

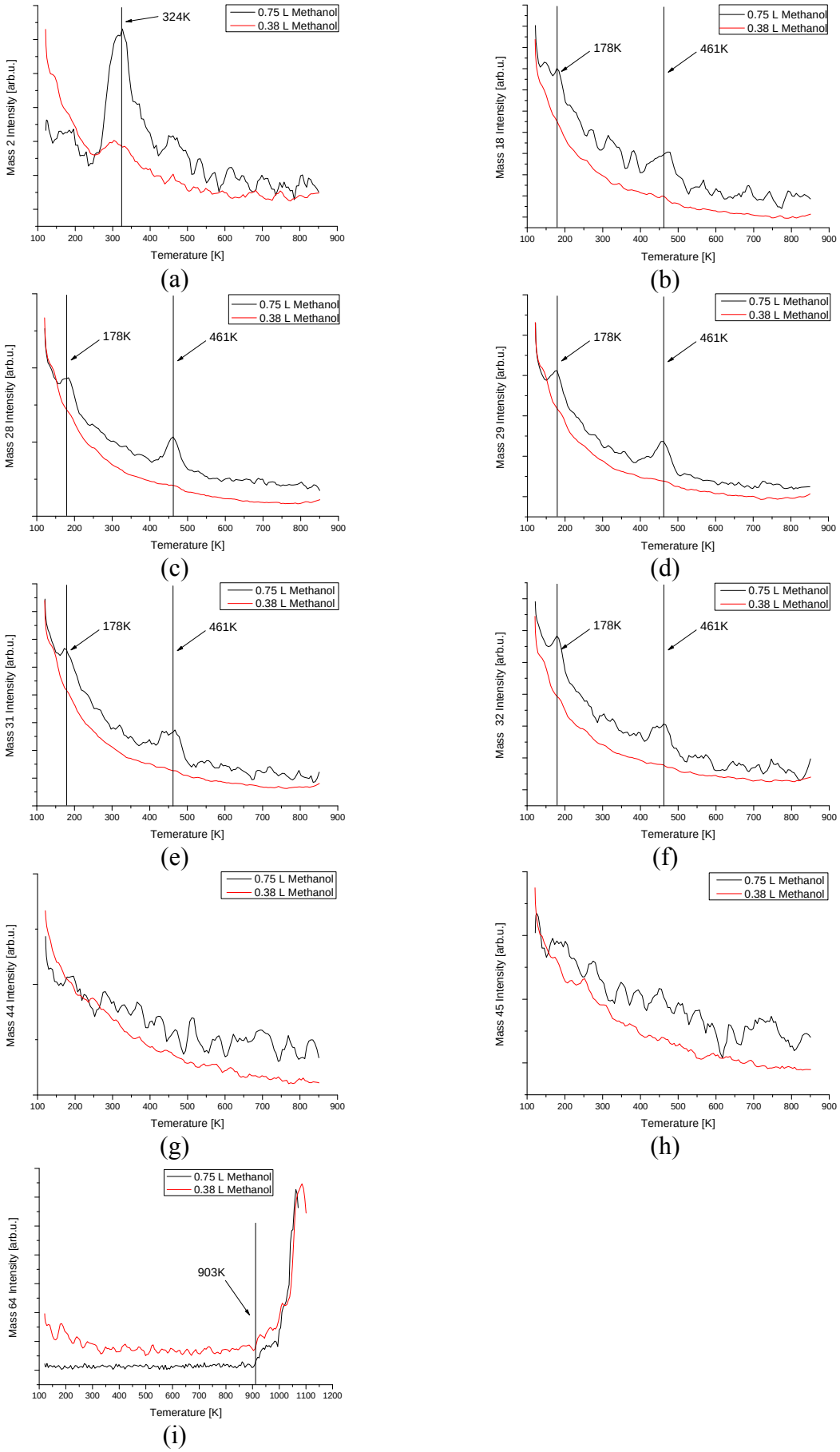

Figure 3.3: Thermal desorption spectra of methanol from Pd/Zn; 0.2 ML zinc, 0.75 L methanol (black line) and 0.4 ML zinc, 0.38 L methanol (red line); (a) mass 2, (b) mass 18, (c) mass 28, (d) mass 29, (e) mass 31, (f) mass 32, (g) mass 44, (h) mass 45, (i) mass 64

Fragmentation or desorption

To determine whether detected mass 18, 28, 29 and 32 show desorption from the surface or are only a methanol fragment, it is necessary to subtract the calculated methanol fragment from the detected spectrum.

First a methanol residual gas spectrum (Figure 3.4) was recorded. Figure 3.5 shows the red marked area in more detail.

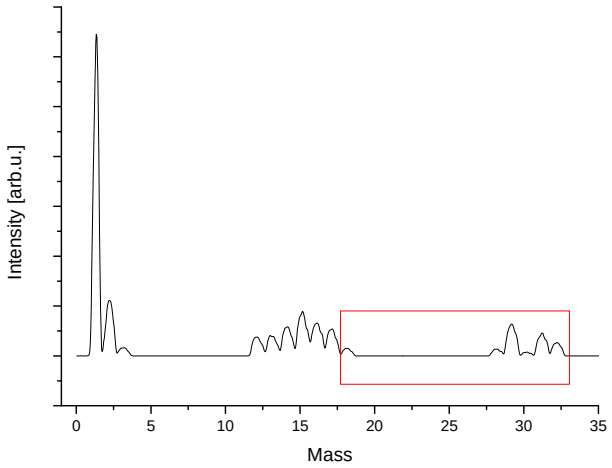

Figure 3.4: Methanol residual gas spectrum

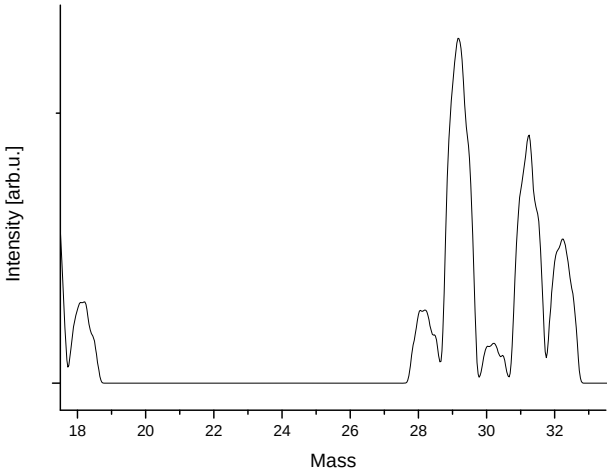

Figure 3.5: Methanol residual gas spectrum in more detail

Table 3.2 shows the measured intensities of the residual gas spectrum. In Table 3.3 the calculated intensity ratio of mass 18, 28, 29, 31 and 32 are seen.

18	28	29	31	32
3,01E-12	2,66E-12	1,28E-11	9,19E-12	5,34E-12

Table 3.2: Absolute intensities

	31
18	0,3274
28	0,2899
29	1,3893
31	1,0000
32	0,5809

Table 3.3: Calculated relative intensities

In Figure 3.6 the calculated methanol fragment (red line) is subtracted from the detected spectrum (black line). The resulting green line shows actual desorption from the sample surface. As can be seen water, carbon monoxide and oxygen show desorption. Formaldehyde however does not desorb. It must be a result of methanol fragmentation in the mass spectrometer.

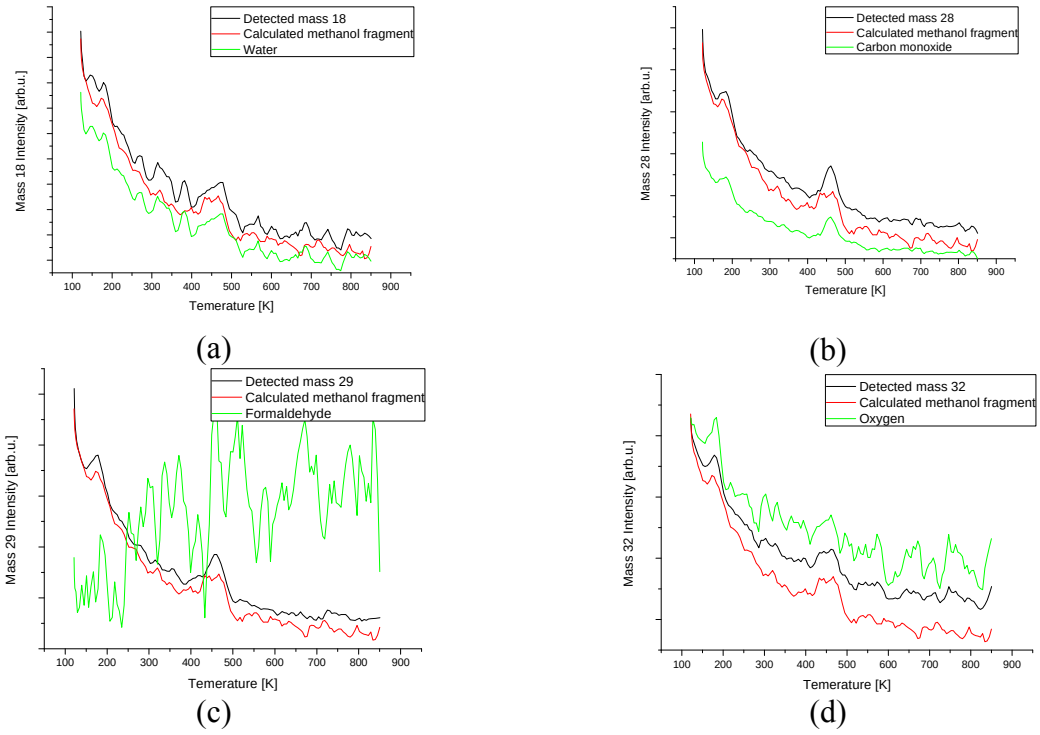

Figure 3.6: Thermal desorption spectra of methanol from Pd/Zn; 0.2 ML zinc, 0.75 L methanol:); (a) mass 18, (b) mass 28, (c) mass 29, (d) mass 32

3.1.2. **Second series of experiments: Pd/ZnO high oxygen pressure**

In the second series of experiments methanol desorption from Pd/ZnO, formed under high oxygen pressure, was investigated. Three experiments were done.

1. 1.4 ML ZnO were deposited on the sample surface at room temperature under an oxygen atmosphere ($1*10^{-5}$ mbar) and the sample was cooled down to 123 K for methanol exposition. A dosage of 1.5 L methanol was given. Figure 3.8 shows the thermal desorption spectra of methanol form Pd/ZnO (red line).

2. 1.4 ML ZnO were deposited on the sample surface at room temperature under an oxygen atmosphere ($1*10^{-5}$ mbar) and the sample was cooled down to 123 K for methanol exposition. A dosage of 1.88 L methanol was given. Figure 3.8 shows the thermal desorption spectra of methanol form Pd/ZnO (blue line).

3. 1.4 ML ZnO were deposited on the sample surface at room temperature under an oxygen atmosphere ($1*10^{-5}$ mbar) and the sample was cooled down to 123 K for methanol exposition. A dosage of 2.28 L methanol was given. Figure 3.8 shows the thermal desorption spectra of methanol form Pd/ZnO (green line).

The resulting sample surface before methanol exposition is shown in Figure 3.7. 1.4 ML Zn deposited under $1*10^{-5}$ mbar oxygen atmosphere forms a monolayer of ZnO (6 x 6) (marked A) which does not completely cover the sample surface (Pd). Additionally triangular shaped islands (bilayer) have grown on the second layer (marked C) [26].

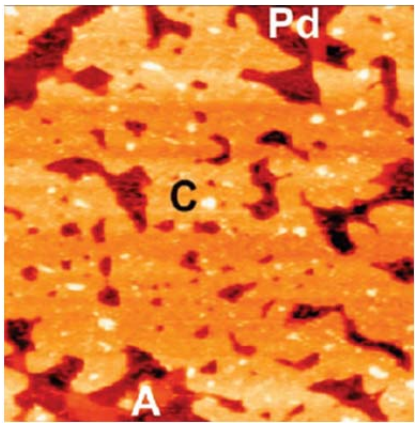

Figure 3.7: STM image (1000 Å x 1000 Å) of 1.4 ML ZnO on Pd (111) formed under $1*10^{-5}$ mbar oxygen atmosphere; adapted from [26]

In Figure 3.8 (a/b/c/d/e/f) the desorption spectra of hydrogen, water/methanol, carbon monoxide, formaldehyde/methanol, methanol and oxygen/methanol (mass 2/18/28/29/31/32) are shown. All experiments show the same desorption at 139 K. The peak is a result of desorbed material from the heating wires holding the crystal. With the increasing methanol dosage a second peak located at 188 K becomes visible that shows desorption from the crystal. In Figure 3.8 (b/c/d/e/f) it seems that the second experiment has higher intensity's than the third experiment, but that is not the case because the spectra have been modified[8] to fit in the plots. The actual signal intensity of experiment three was higher than in the second experiment.

[8] Origin layers were scaled in height

In Figure 3.8 (g/h) the desorption spectra of carbon dioxide and formate is shown. As can be seen one peak at 348 K becomes visible with higher methanol dosage.

Figure 3.8 (i) shows the desorption spectrum of zinc. All three experiments show Zinc desorption starting at 877 K which is where it is expected to be [5] considering the temperature-measurement-error.

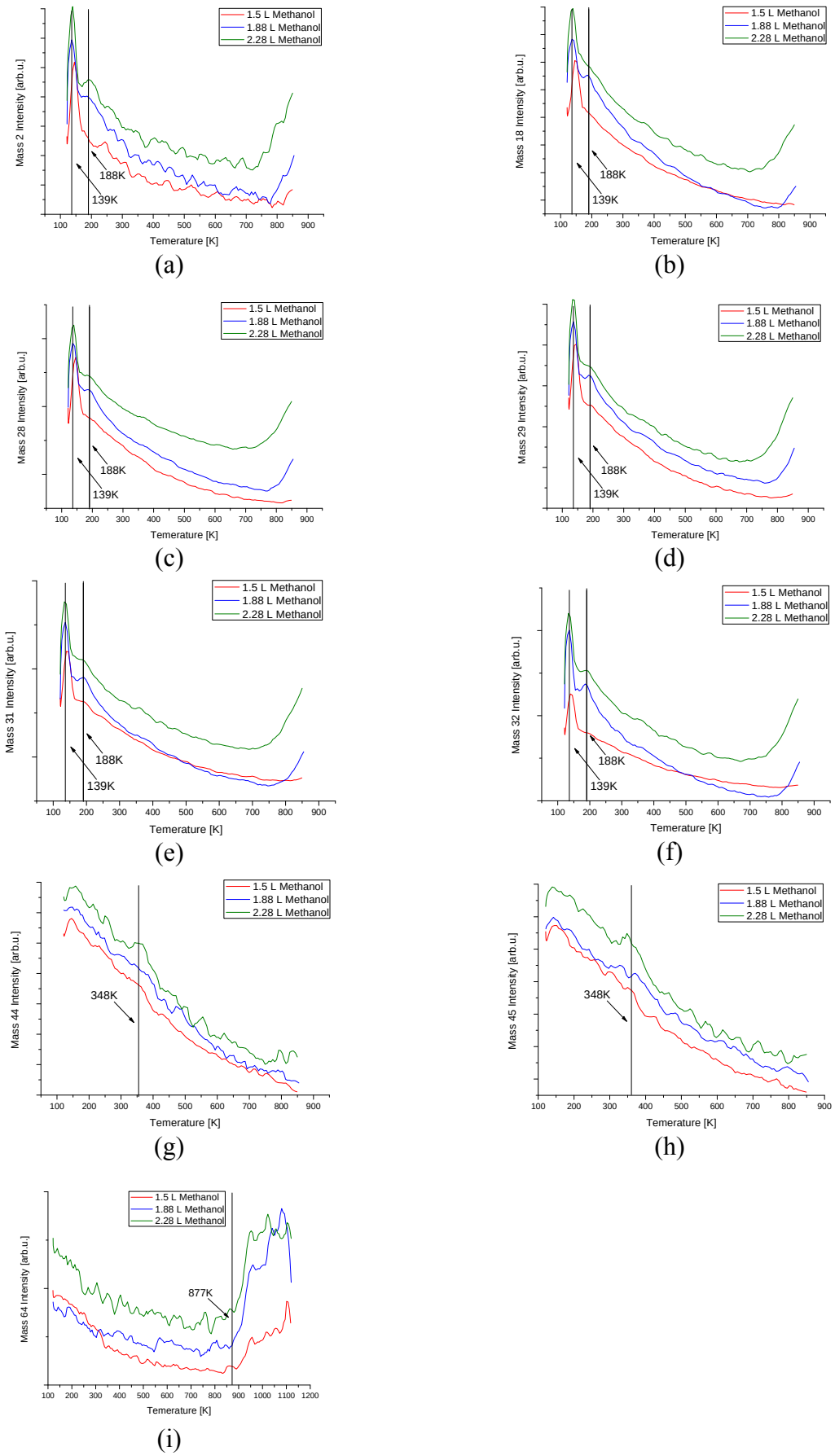

Figure 3.8: Thermal desorption spectra of methanol from Pd/ZnO; 1.4 ML ZnO (O pressure $1*10^{-5}$ mbar), 1.5 L / 1.88 L / 2.28 L methanol exposure; (a) mass 2, (b) mass 18, (c) mass 28, (d) mass 29, (e) mass 31, (f) mass 32, (g) mass 44, (h) mass 45, (i) mass 64

3.1.3. Third series of experiments: Pd/ZnO low oxygen pressure

In the third series of experiments methanol desorption from Pd/ZnO, formed under low oxygen pressure, was investigated. Three experiments with different methanol dosages were done.

1. 1.4 ML ZnO were deposited on the sample surface at room temperature under an oxygen atmosphere ($1*10^{-7}$ mbar). Then the sample was cooled down to 123 K for methanol exposition. A dosage of 1.13 L methanol was given. Figure 3.10 shows the thermal desorption spectra of methanol form Pd/ZnO (blue line).

2. 1.4 ML ZnO were deposited on the sample surface at room temperature under an oxygen atmosphere ($1*10^{-7}$ mbar). Then the sample was cooled down to 123 K for methanol exposition. A dosage of 1.5 L methanol was given. Figure 3.10 shows the thermal desorption spectra of methanol form Pd/ZnO (green line).

3. 1.4 ML ZnO were deposited on the sample surface at room temperature under an oxygen atmosphere ($1*10^{-7}$ mbar). Then the sample was cooled down to 123 K for methanol exposition. A dosage of 2.26 L methanol was given. Figure 3.10 shows the thermal desorption spectra of methanol form Pd/ZnO (red line).

The resulting sample surface before methanol exposition is shown in Figure 3.9. 1.4 ML Zn deposited under $1*10^{-7}$ mbar oxygen atmosphere forms a monolayer of ZnO (6 x 6) (marked A) which does not completely cover the sample surface (black areas). Additionally triangular shaped islands (marked C) and hexagonal shaped islands (marked B) have grown on the second layer [26].

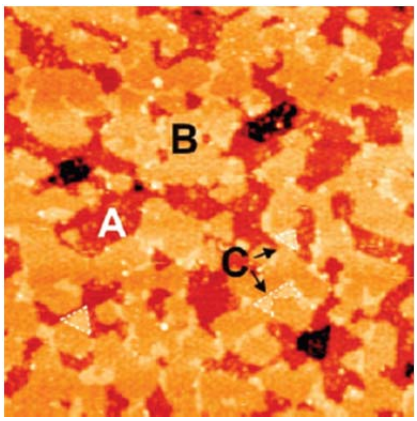

Figure 3.9: STM image (1000 Å x 1000 Å) of 1.4 ML ZnO on Pd (111) formed under $1*10^{-7}$ mbar oxygen atmosphere; adapted from [26]

The desorption spectra of hydrogen are shown in Figure 3.10 (a). The first peak seen at 135 K is a result of desorbed material from the heating wires holding the crystal. A second peak at 196 K can only be seen clearly in the green line (1.5 ML). In the other two experiments the rather high signal to noise ratio makes it impossible to say if or at what temperature hydrogen desorption occurs from the sample surface.

In Figure 3.10 (b/c/d/e/f) the desorption spectra of water/methanol, carbon monoxide, formaldehyde/methanol, methanol and oxygen/methanol (mass 18/28/29/31/32) are shown. They all show the same curve shape. Three peaks at the exact same temperature can be seen for each single mass. The first peak at 135 K, at the beginning of each spectra, is a result of

desorbed material from the heating wires holding the crystal. The second peak at 196 K and the third peak at 389 show the desorption from the crystal.

In Figure 3.10 (g/h) the desorption spectra of carbon dioxide and formate are shown. The spectrum of carbon dioxide (mass 44) shows a peak at 382 K and the one from formate (mass 45) a peak at 397 K.

Figure 3.10 (i) shows the desorption spectrum of zinc. Zinc desorption starts at 860 K which is where it is expected to be [5] considering the temperature-measurement-error.

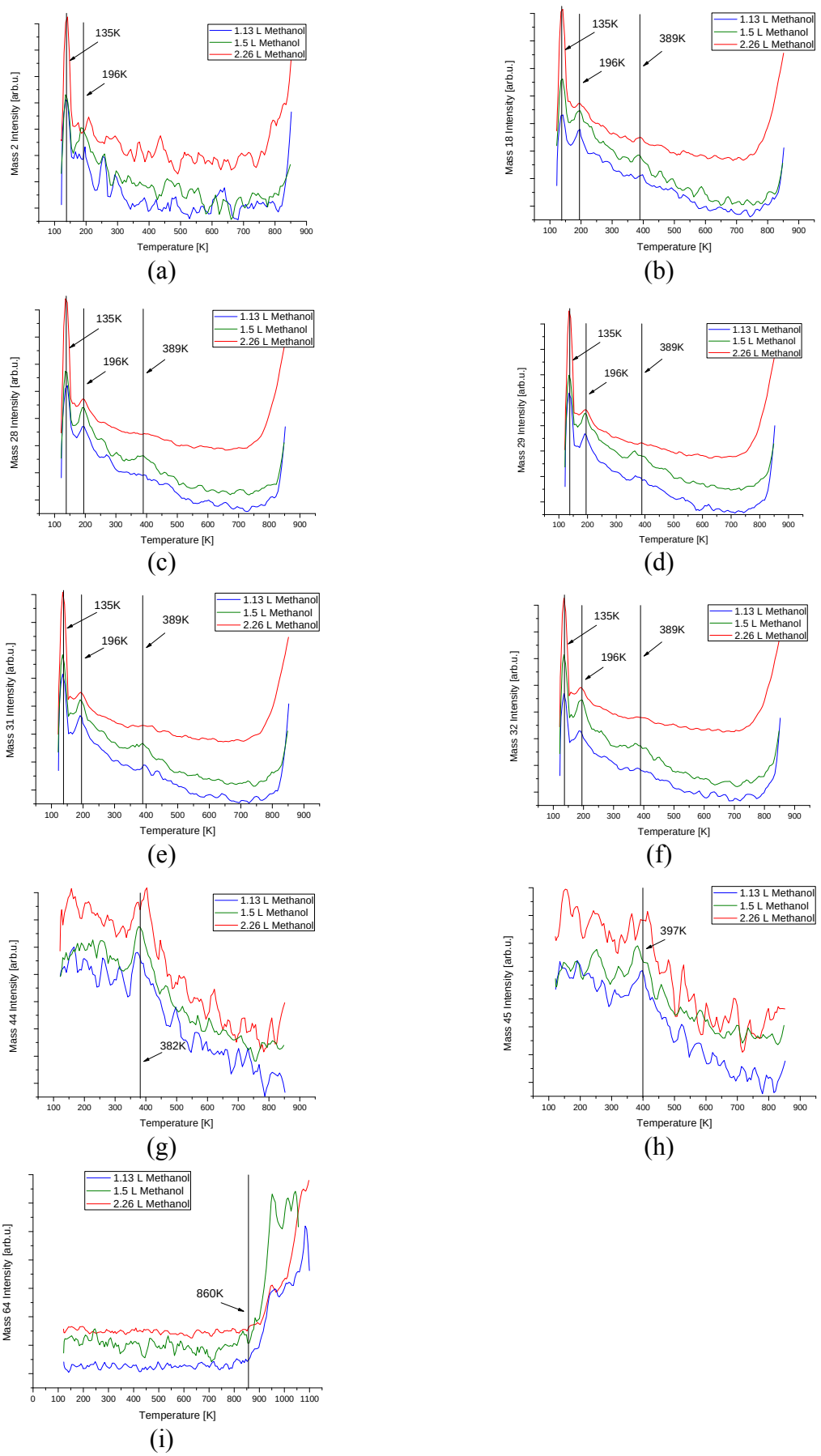

Figure 3.10: Thermal desorption spectra of methanol from Pd/ZnO; 1.4 ML ZnO (O pressure 1*10^{-7} mbar), 1.13 L / 1.5 L / 2.26 L methanol exposure; (a) mass 2, (b) mass 18, (c) mass 28, (d) mass 29, (e) mass 31, (f) mass 32, (g) mass 44, (h) mass 45, (i) mass 64

Fragmentation or desorption

To determine whether detected masses 18, 28, 29 and 32 show desorption from the surface or are only a methanol fragment, it is necessary to subtract the calculated methanol fragment from the detected spectrum.

Table 3.4 shows the measured intensities of the residual gas spectrum. In Table 3.5 the calculated intensity ratio of mass 18, 28, 29, 31 and 32 are seen.

18	28	29	31	32
3,01E-12	2,66E-12	1,28E-11	9,19E-12	5,34E-12

Table 3.4: Absolute intensities

	31
18	0,3274
28	0,2899
29	1,3893
31	1,0000
32	0,5809

Table 3.5: Calculated relative intensities

In Figure 3.6 the calculated methanol fragment (red line) is subtracted from the detected spectrum (black line). The resulting green line shows actual desorption from the sample surface. As can be seen water, carbon monoxide, formaldehyde and oxygen show desorption.

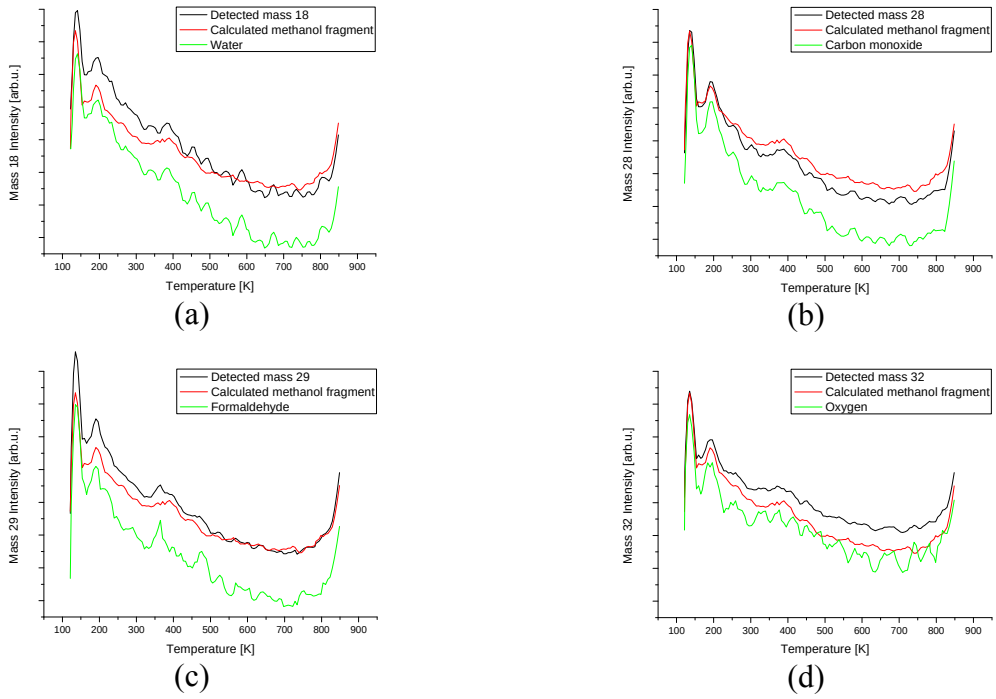

Figure 3.11: Thermal desorption spectra of methanol from Pd/Zn; 1.4 ML zinc, 1.5 L methanol:); (a) mass 18, (b) mass 28, (c) mass 29, (d) mass 32

3.1.4. **Discussion - Methanol desorption from Pd/Zn and Pd/ZnO**

In the following chapter one representative experiment of each series of experiments was chosen to show the different methanol reactions as a result of the production process of the Zn films.

Methanol desorption from three different Pd/(ZnO) films are compared:

Series 1: Methanol 0.75 L; Zn 0.2 ML
Series 2: Methanol 1.88 L; ZnO 1.4 ML (high O pressure)
Series 3: Methanol 1.13 L; ZnO 1.4 ML (low O pressure)

Additionally desorption from a clean Pd (111) surface covered by 1.25 ML methanol is shown for mass 2, 18, 28 and 31 [27].

To make the comparison easier to visualize all spectra of one mass are shown in one plot. It should be noted that the intensities of each single curve must not be compared to the others because their scale was adjusted to fit in the plot.

In Figure 3.12 (a) hydrogen desorption is shown. There is one apparent resemblance between series two (Methanol 1.88 L; ZnO 1.4 ML (high pressure)) and three (Methanol 1.13 L; ZnO 1.4 ML (low pressure)). Both show hydrogen desorption at approximately 139 K and 179 K. Hydrogen desorption form Pd/Zn (Methanol 0.75 L; Zn 0.2 ML) is very similar to desorption from clean Pd (Methanol 1.25 L). Both show high temperature hydrogen desorption at about 324 K.

Figure 3.12 (b) shows the desorption of water from the sample surface. Series two (Methanol 1.88 L; ZnO 1.4 ML (high pressure)) and three (Methanol 1.13 L; ZnO 1.4 ML (low pressure)) show the same peaks located at approximately 140 K and 196 K. Series one also seems to have a desorption peak at 196 K, but due to signal noise ratio this is hard to tell. Whereas the second peak at 368 K is clearly visible whereas water desorption from clean Pd (Methanol 1.25 L) seems to only happen at 154 K. Beyond 805 K water starts to desorb from the sample holder.

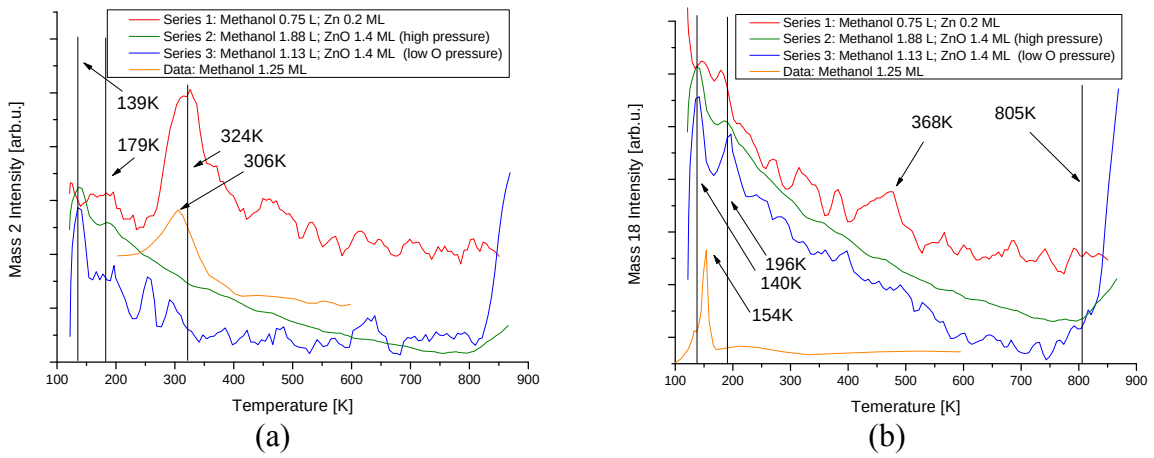

Figure 3.12: Comparison Mass 2 (a) and Mass 18 (b)

In Figure 3.13 (a) carbon monoxide and methanol (fragment) desorption is shown. Series two (Methanol 1.88 L; ZnO 1.4 ML (high pressure)) and three (Methanol 1.13 L; ZnO 1.4 ML (low pressure)) share a peak located at 139 K. It should also be visible in series one because it shows desorption from the sample holder, but due to the very small dosage of methanol in this experiment no such desorption was measured. All three series show low temperature desorption at 179 K. Series one additionally shows high temperature desorption at 461 K which very well corresponds with desorption from clean Pd (Methanol 1.25 L) that shows a peak at 485 K.

In Figure 3.13 (b) formaldehyde and methanol (fragment) is shown. Measurements are very similar to the results shown in Figure 3.13 (a). Series two (Methanol 1.88 L; ZnO 1.4 ML (high pressure)) and three (Methanol 1.13 L; ZnO 1.4 ML (low pressure)) share a peak located at 139 K. Each series shows low temperature desorption at 179 K. Series one (Methanol 0.75 L; Zn 0.2 ML) also shows high temperature peak at 461 K. But as can be seen in chapter 3.1.1 on page 28 both peaks (high and low temperature) shown by series one are a result of fragmentation of methanol in the mass detector.

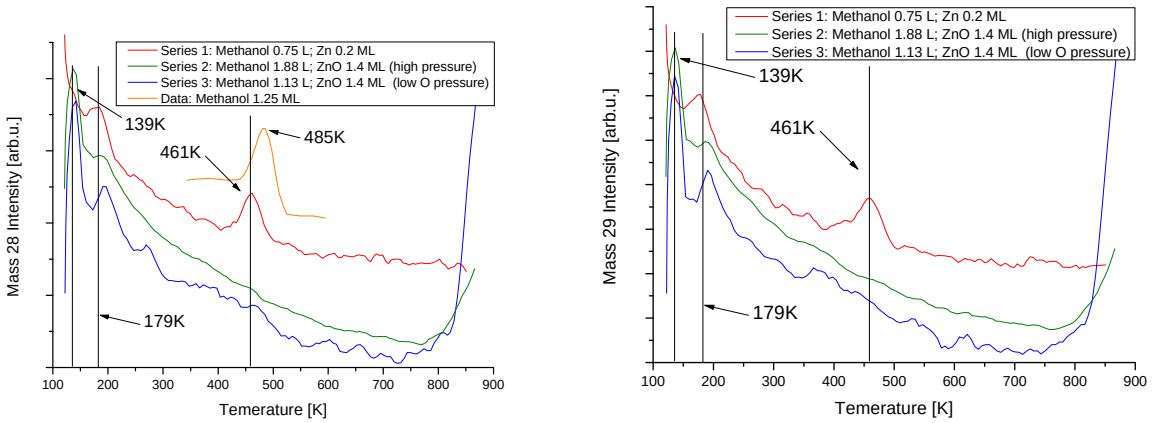

Figure 3.13: Comparison Mass 28 (a) and Mass 29 (b)

In Figure 3.14 (a) methanol desorption is shown. Series two (Methanol 1.88 L; ZnO 1.4 ML (high pressure)) and three (Methanol 1.13 L; ZnO 1.4 ML (low pressure)) share a peak located at 139 K. At this temperature methanol also desorbs from clean Pd (Methanol 1.25 L). It additionally shows a small peak at 153 K but no high temperature desorption can be seen. Each series shows low temperature desorption at 179 K but only experiment one (Methanol 0.75 L; Zn 0.2 ML) shows high temperature desorption at 461 K.

In Figure 3.14 (b) oxygen and methanol is shown. Measurements are very similar to the results shown in Figure 3.14 (a). Experiment two (Methanol 1.88 L; ZnO 1.4 ML (high pressure)) and three (Methanol 1.13 L; ZnO 1.4 ML (low pressure)) share a peak located at 139 K. Each series shows low temperature desorption at 179 K but only series one (Methanol 0.75 L; Zn 0.2 ML) additionally shows high temperature desorption at 461 K. It is not the result of fragmentation in the mass spectrometer (see page 28).

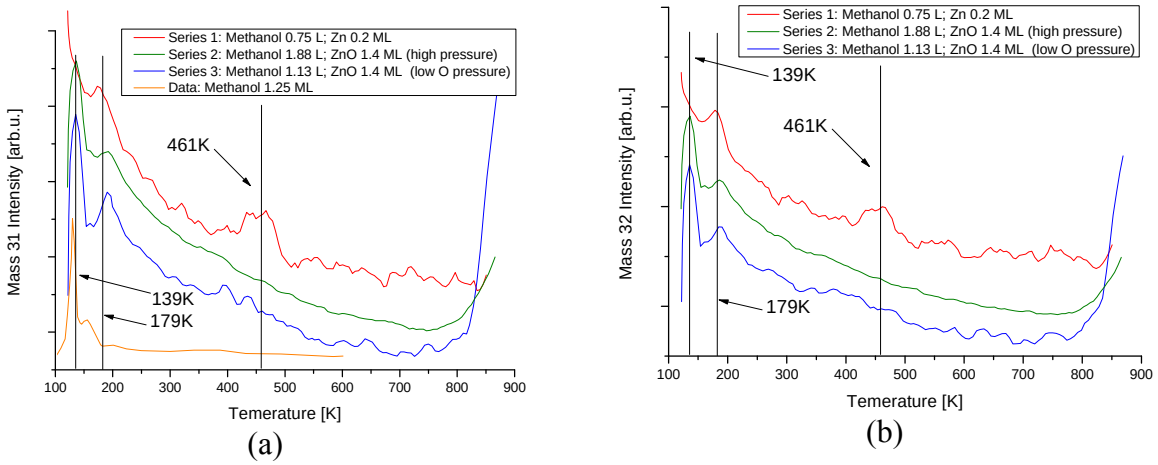

Figure 3.14: Comparison Mass 31 (a) and Mass 32 (b)

In Figure 3.15 (a) desorption of carbon dioxide from the sample surface is shown. Only series three (Methanol 1.13 L; ZnO 1.4 ML (low pressure)) shows a peak located at 372 K. Series one (Methanol 0.75 L; Zn 0.2 ML) and two (Methanol 1.88 L; ZnO 1.4 ML (high pressure)) show no desorption at all. Although the rather high signal to noise ratio in experiment one makes it difficult to be absolutely sure.

In Figure 3.15 (b) formate desorption is shown. Measurements are very similar to the results shown in Figure 3.15 (a). Again only series three (Methanol 1.13 L; ZnO 1.4 ML (low pressure)) shows a peak located at 399 K. Series one (Methanol 0.75 L; Zn 0.2 ML) and two (Methanol 1.88 L; ZnO 1.4 ML (high pressure)) show no desorption during the heating process.

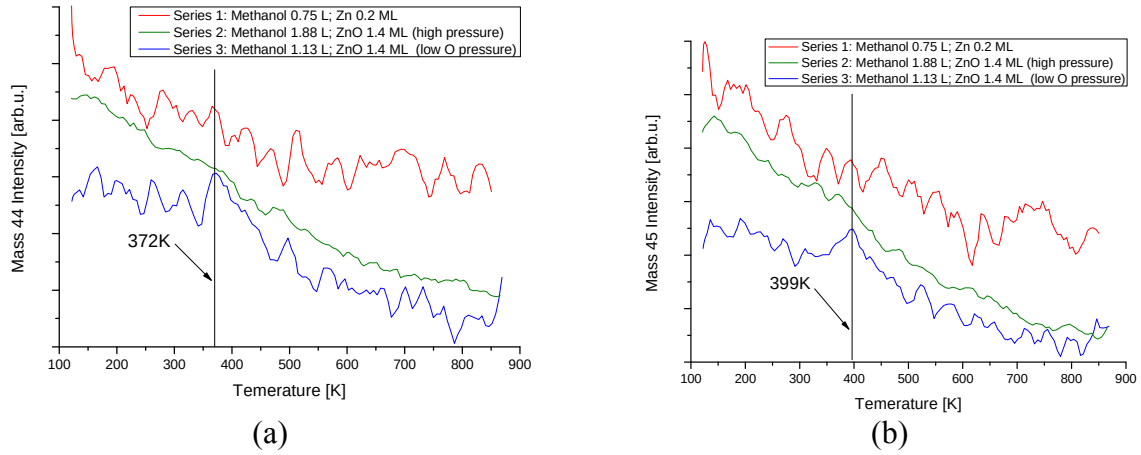

Figure 3.15: Comparison Mass 44 (a) and Mass 45 (b)

In Figure 3.16 (a) zinc desorption is shown. In series one (Methanol 0.75 L; Zn 0.2 ML) zinc without oxygen impurities starts to desorb from the palladium crystal at approximately 903 K, whereas in series two (Methanol 1.88 L; ZnO 1.4 ML (high pressure)) and three (Methanol 1.13 L; ZnO 1.4 ML (low pressure)) the zinc oxide layer already starts to desorb at 845 K.

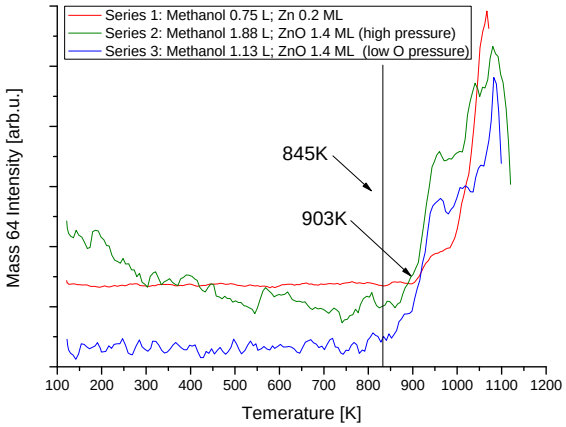

Figure 3.16: Comparison Mass 64

3.2. Methanol desorption from ultra-thin ZnO layers

3.2.1. First series of experiments: Pd/ZnO low oxygen pressure

In the first series of experiments methanol desorption from Pd/ZnO, formed under low oxygen pressure, was investigated. Five experiments with the exact same settings were done.

1. 0.35 ML ZnO were deposited on the sample surface at room temperature under an oxygen atmosphere ($1*10^{-8}$ mbar). Then the sample was cooled down to 123 K for methanol exposition. A dosage of 0.56 L methanol was given. Figure 3.18 shows the thermal desorption spectra of methanol form Pd/ZnO.

The resulting sample surface before methanol exposition is shown in Figure 3.17. 0.35 ML Zn deposited under $1*10^{-8}$ mbar oxygen atmosphere forms a Pd(111) surface covered by (4 x 4) and (6 x 6) structured ZnO islands [26].

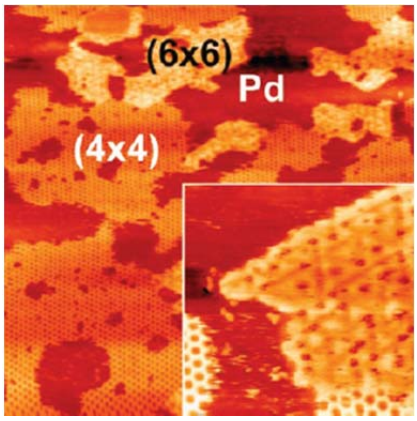

Figure 3.17: STM image (1000 Å x 1000 Å) of ~0.6-0.7 ML ZnO on Pd (111) formed under $1*10^{-8}$ mbar oxygen atmosphere [inset (200 Å x 200 Å)];
adapted from [26]

The desorption spectra of hydrogen are shown in Figure 3.18 (a). No hydrogen desorption from the crystal was detected.

In Figure 3.18 (b/c/d/e/f) the desorption spectra of water/methanol, carbon monoxide, formaldehyde/methanol, methanol and oxygen/methanol (mass 18/28/29/31/32) are shown. They all show the same curve shape. Two peaks at the exact same temperature can be seen. The first peak has its maximum at 219 K and the second at 372 K.

In Figure 3.18 (g/h) the desorption spectra of carbon dioxide and formate (mass 44/45) are shown. Both spectra show a peak located at 372 K.

Figure 3.18 (i) shows the desorption spectrum of zinc (mass 64). The zinc desorption starts at 916 K.

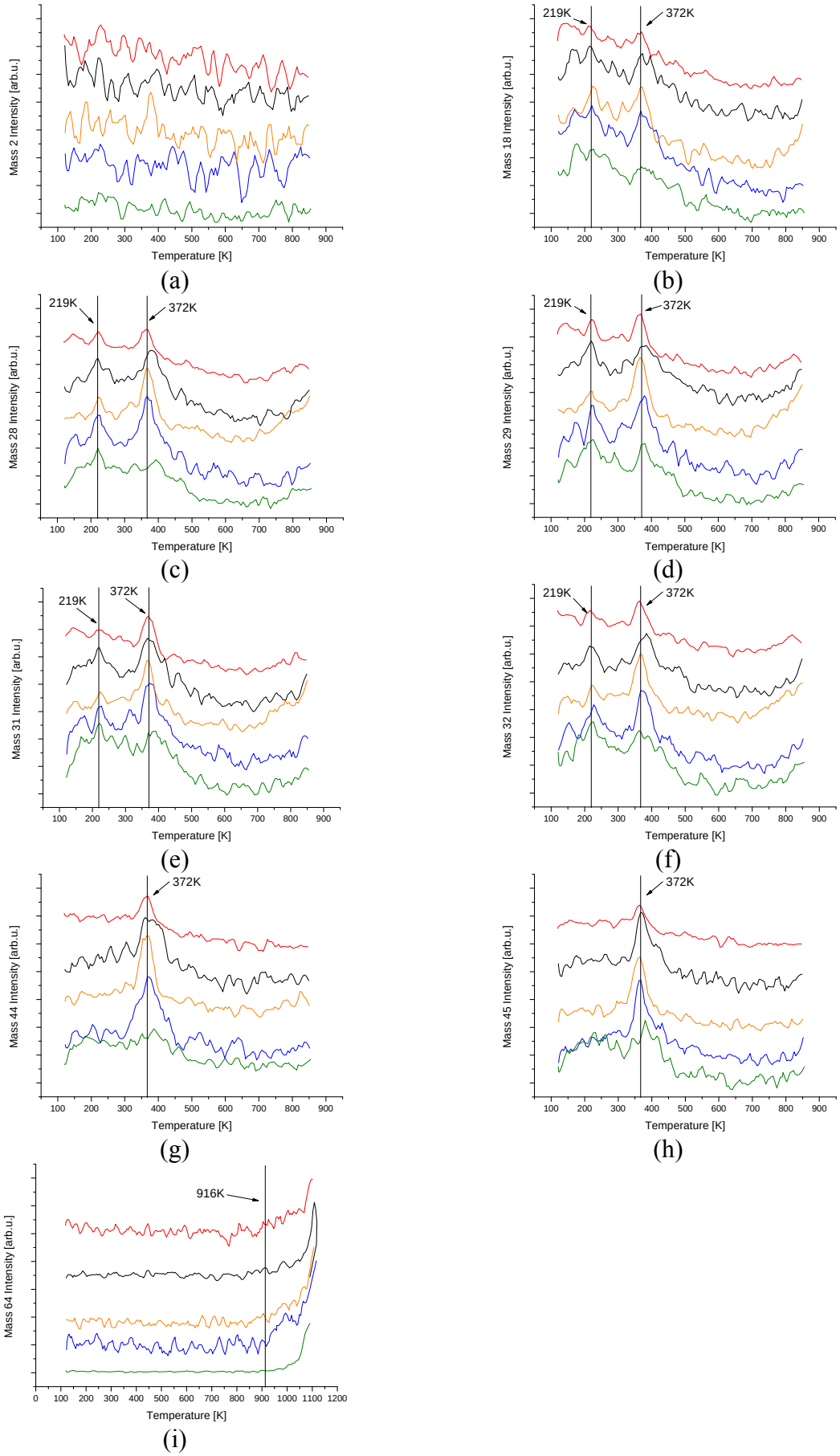

Figure 3.18: Thermal desorption spectra of methanol from Pd/ZnO; 0.35 ML ZnO (O pressure $1*10^{-8}$ mbar), 0.56 L methanol exposure; (a) mass 2, (b) mass 18, (c) mass 28, (d) mass 29, (e) mass 31, (f) mass 32, (g) mass 44, (h) mass 45, (i) mass 64

Fragmentation or desorption

To determine whether detected masses 18, 28, 29 and 32 show desorption from the surface or are only a methanol fragment, it is necessary to subtract the calculated methanol fragment from the detected spectrum.

Table 3.6 shows the measured intensities of the residual gas spectrum. In Table 3.7 the calculated intensity ratio of mass 18, 28, 29, 31 and 32 are seen.

18	28	29	31	32
3,01E-12	2,66E-12	1,28E-11	9,19E-12	5,34E-12

Table 3.6: Absolute intensities

	31
18	0,3274
28	0,2899
29	1,3893
31	1,0000
32	0,5809

Table 3.7: Calculated relative intensities

In Figure 3.6 the calculated methanol fragment (red line) is subtracted from the detected spectrum (black line). The resulting green line shows actual desorption from the sample surface. As can be seen water, carbon monoxide and oxygen show desorption. Formaldehyde however does not desorb. It must be a result of methanol fragmentation in the mass spectrometer.

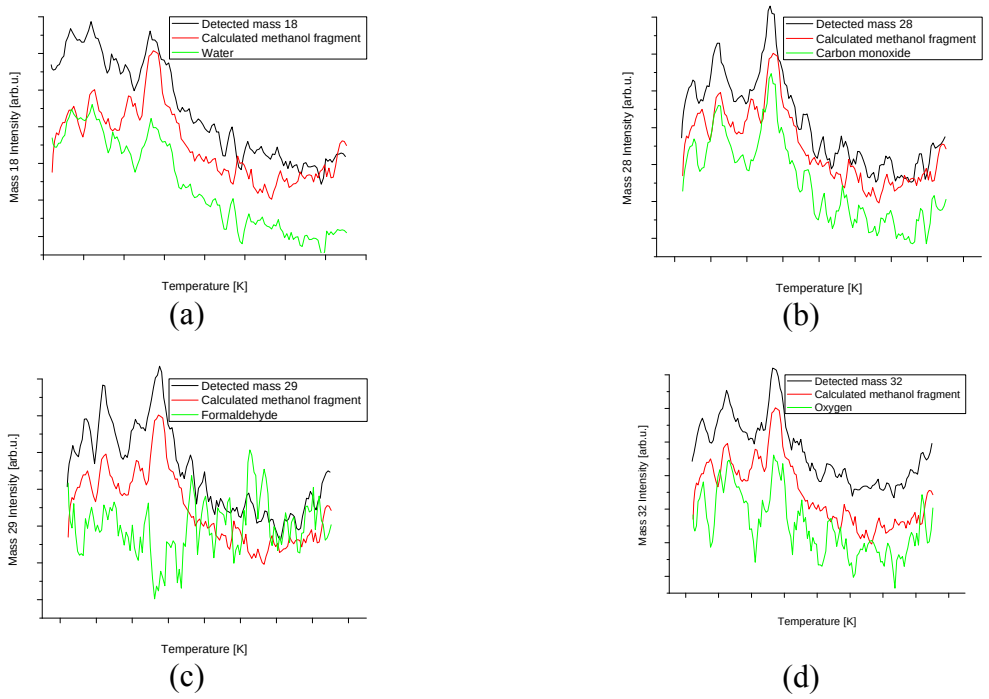

Figure 3.19: Thermal desorption spectra of methanol from Pd/Zn; 0.35 ML zinc, 0.56 L methanol:); (a) mass 18, (b) mass 28, (c) mass 29, (d) mass 32

3.2.2. **Second series of experiments: Pd/ZnO low oxygen pressure**

In the second series of experiments methanol desorption from Pd/ZnO, formed under low oxygen pressure, was investigated. Two experiments were done:

1. 0.35 ML ZnO were deposited on the sample surface at room temperature under an oxygen atmosphere ($1*10^{-8}$ mbar). Then the sample was cooled down to 123 K for methanol exposition. A dosage of 0.56 L methanol was given. Figure 3.20 shows the thermal desorption spectra of methanol form Pd/ZnO.

2. 0.7 ML ZnO were deposited on the sample surface at room temperature under an oxygen atmosphere ($1*10^{-8}$ mbar). Then the sample was cooled down to 123 K for methanol exposition. A dosage of 0.56 L methanol was given. Figure 3.20 shows the thermal desorption spectra of methanol form Pd/ZnO.

The resulting sample surface before methanol exposition is shown in Figure 3.17 on page 40. Sub ML Zn deposited under $1*10^{-8}$ mbar oxygen atmosphere forms a Pd(111) surface covered by (4 x 4) and (6 x 6) structured ZnO islands [26].

The desorption spectra of hydrogen are shown in Figure 3.20 (a). Hydrogen desorption reaches its maximum at 193 K. Experiment one shows a clear peak at this temperature where the peak of experiment two is way smaller.

In Figure 3.20 (b/c/d/e/f/) the desorption spectra of water/methanol, carbon monoxide, formaldehyde/methanol, methanol and oxygen/methanol (mass 18/28/29/31/32) are shown. They all show the same curve shape. There are always two low temperature peaks at 152 K and 193K. The high temperature peak is well defined in experiment two at 456 K. Experiment one shows more broadened desorption between 380 K and 460 K. Mass 32 (Figure 3.20 (f)) even shows its highest high temperature peak at 380 K.

In Figure 3.20 (g/h) the desorption spectra of carbon dioxide and formate (mass 44/45) are shown. In both experiments two peaks for each mass are seen, although the maxima of carbon dioxide and formate are not at the same position. Maximum desorption of carbon dioxide can be seen at 251 and 392 K whereas formate desorbs at 245 k and 403 K.

Figure 3.20 (i) shows the desorption spectrum of zinc. Zinc desorption starts at 920 K.

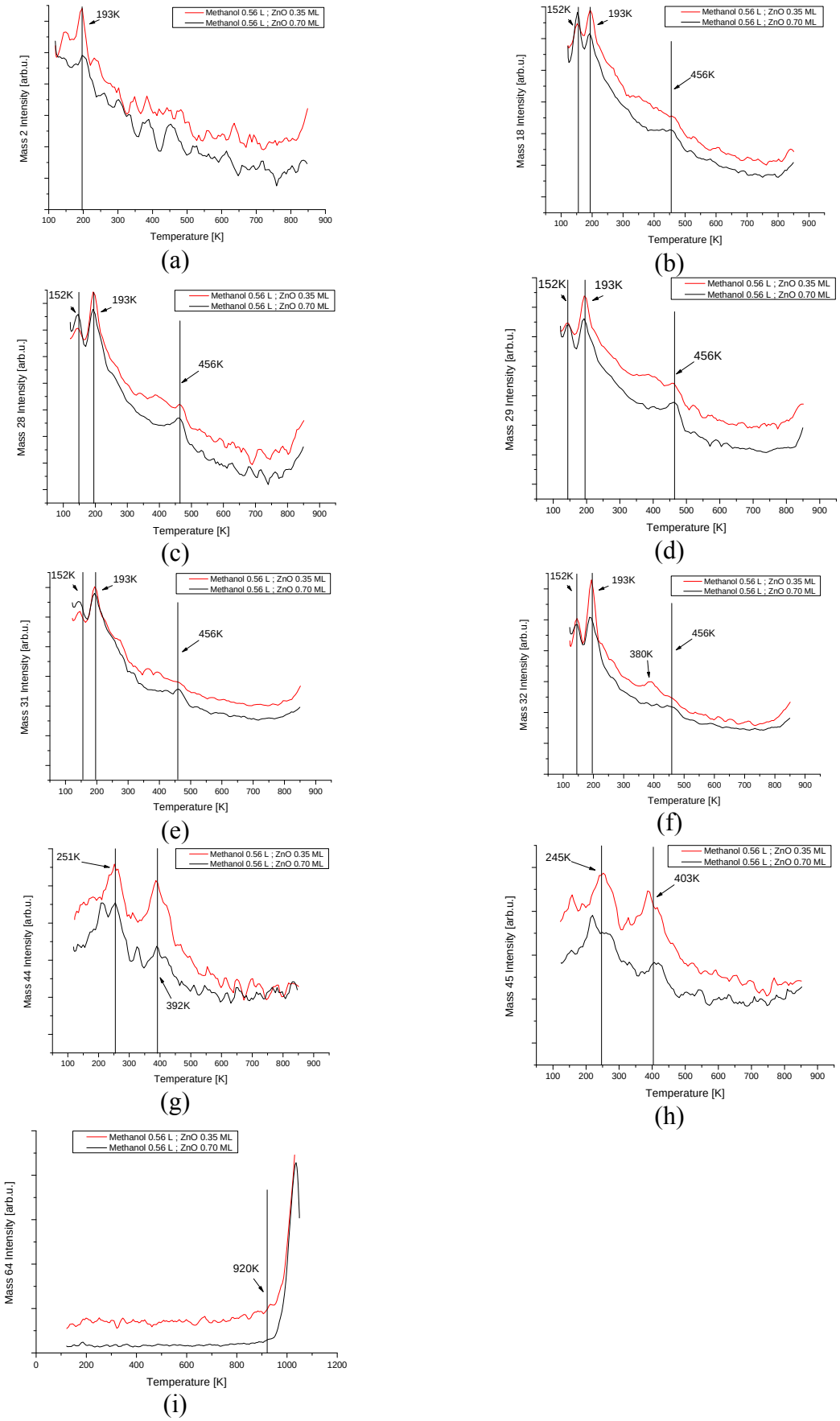

Figure 3.20: Thermal desorption spectra of methanol from Pd/ZnO; 0.35 / 0.7 ML ZnO (O pressure 1*10^{-8} mbar), both experiments with 0.56 L methanol exposure; (a) mass 2, (b) mass 18, (c) mass 28, (d) mass 29, (e) mass 31, (f) mass 32, (g) mass 44, (h) mass 45, (i) mass 64

Fragmentation or desorption

To determine whether detected masses 18, 28, 29 and 32 show desorption from the surface or are only a methanol fragment, it is necessary to subtract the calculated methanol fragment from the detected spectrum.

Table 3.8 shows the measured intensities of the residual gas spectrum. In Table 3.9 the calculated intensity ratio of mass 18, 28, 29, 31 and 32 are seen.

18	28	29	31	32
3,01E-12	2,66E-12	1,28E-11	9,19E-12	5,34E-12

Table 3.8: Absolute intensities

	31
18	0,3274
28	0,2899
29	1,3893
31	1,0000
32	0,5809

Table 3.9: Calculated relative intensities

In Figure 3.6 the calculated methanol fragment (red line) is subtracted from the detected spectrum (black line). The resulting green line shows actual desorption from the sample surface. Water and carbon monoxide show high and low temperature desorption. The calculated result of Oxygen only shows low temperature desorption. Formaldehyde however does not desorb. It must be a result of methanol fragmentation in the mass spectrometer.

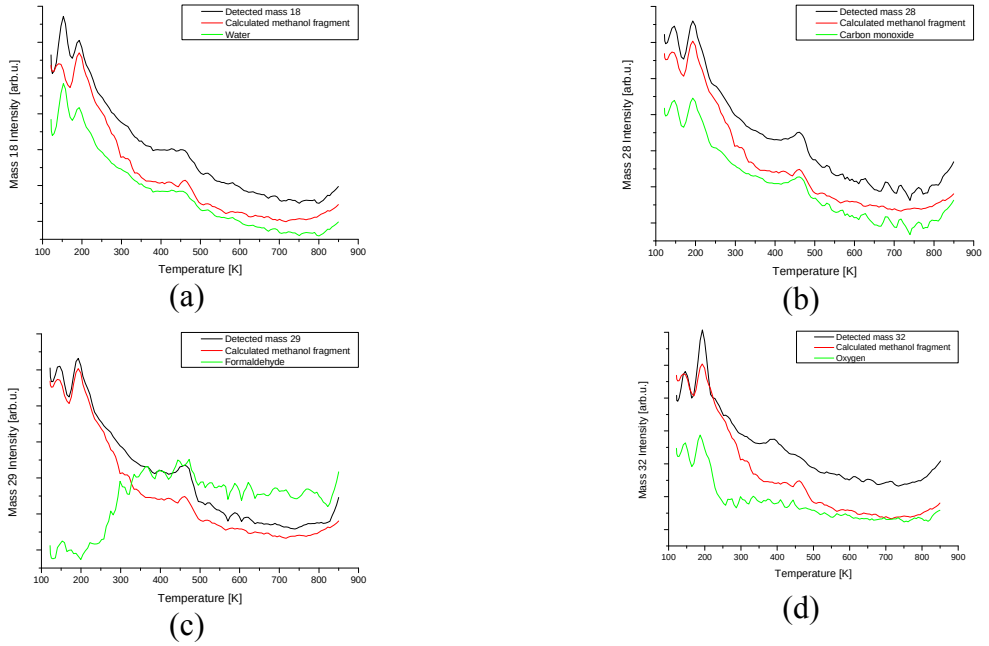

Figure 3.21: Thermal desorption spectra of methanol from Pd/Zn; 0.70 ML zinc, 0.56 L methanol:); (a) mass 18, (b) mass 28, (c) mass 29, (d) mass 32

3.2.3. **Third series of experiments: Pd/ZnO low oxygen pressure**

In the third series of experiments methanol desorption from Pd/ZnO, formed under low oxygen pressure, was investigated. Two experiments under the same conditions were done:

1. 0.35 ML ZnO were deposited on the sample surface at room temperature under an oxygen atmosphere ($1*10^{-8}$ mbar). Then the sample was cooled down to 123 K for methanol exposition. A dosage of 0.04 L methanol was given. Figure 3.22 shows the thermal desorption spectra of methanol form Pd/ZnO.

The resulting sample surface before methanol exposition is shown in Figure 3.17 on page 40. 0.35 ML Zn deposited under $1*10^{-8}$ mbar oxygen atmosphere forms a Pd(111) surface covered by (4 x 4) and (6 x 6) structured ZnO islands [26].

The desorption spectra of hydrogen are shown in Figure 3.22 (a). Hydrogen desorption at 200 K was detected only in one of the two experiments.

In Figure 3.22 (b) desorption of water/methanol is shown. Both experiments share their peak positions at 152 K, 193 K and 456 K.

In Figure 3.22 (c/d/e/f/) the desorption spectra of carbon monoxide, formaldehyde/methanol, methanol and oxygen/methanol (mass 18/28/29/31/32) are shown. Both experiments do always show two peaks although the position of the first one shifted for approximately 18 K from one experiment to the other. The second peak is seen at 456 K and the peak intensities are reversed. In one experiment the first peak is the higher one while in the other experiment the second one is higher.

In Figure 3.22 (g/h) the desorption spectra of carbon dioxide and formate (mass 44/45) are shown. Both experiments show two peaks for each mass, although the maxima of carbon dioxide and formate are not at the same position. Maximum desorption of carbon dioxide can be seen at 261 and 419 K whereas formate desorbs at 262 k and 403 K.

Figure 3.22 (i) shows the desorption spectrum of zinc. Zinc desorption starts at 920 K.

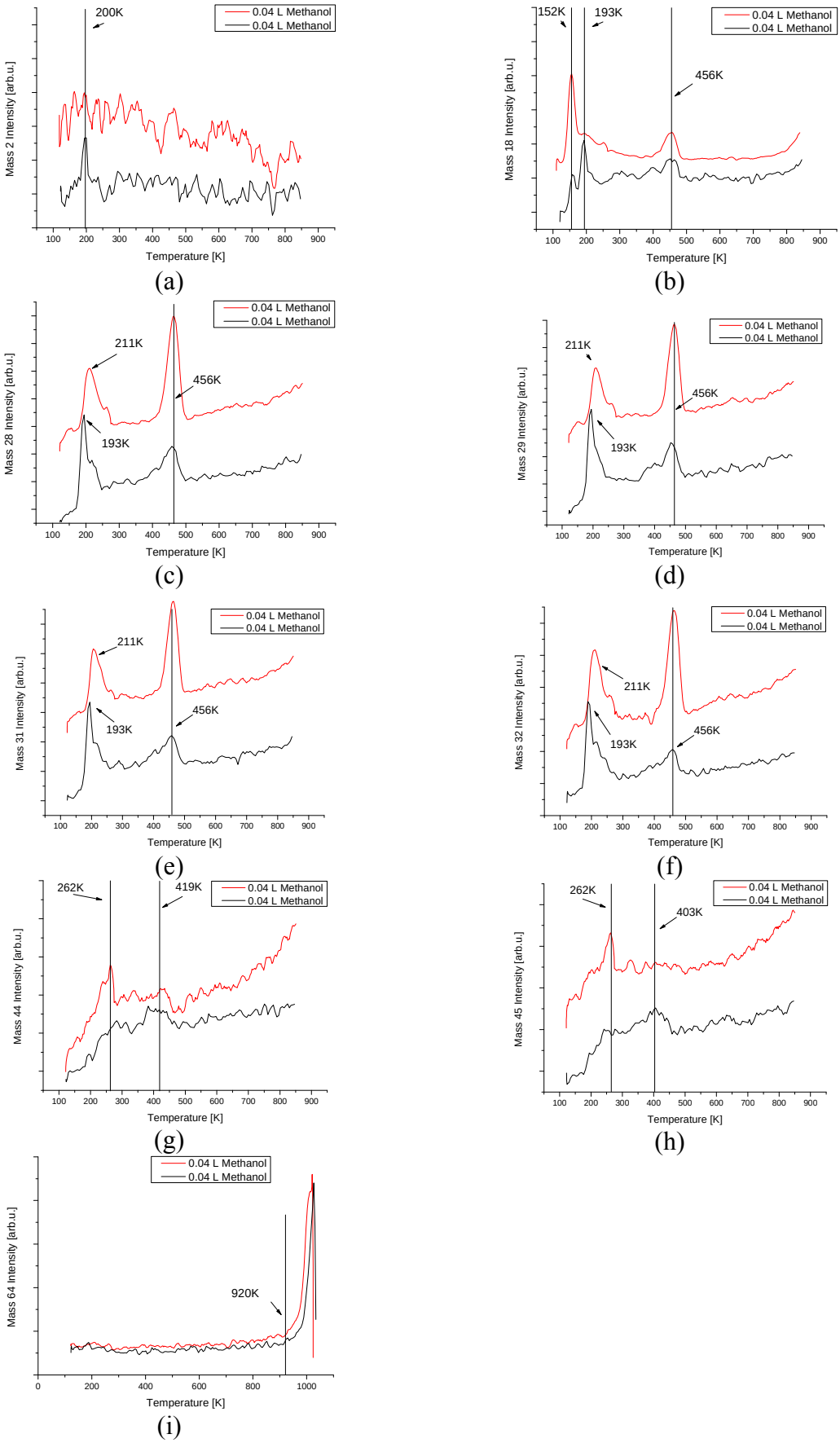

Figure 3.22: Thermal desorption spectra of methanol from Pd/ZnO; 0.35 ML ZnO (O pressure 1*10^{-8} mbar), two experiments with 0.04 L methanol exposure; (a) mass 2, (b) mass 18, (c) mass 28, (d) mass 29, (e) mass 31, (f) mass 32, (g) mass 44, (h) mass 45, (i) mass 64

Fragmentation or desorption

To determine whether detected masses 18, 28, 29 and 32 show desorption from the surface or are only a methanol fragment, it is necessary to subtract the calculated methanol fragment from the detected spectrum.

Table 3.10 shows the measured intensities of the residual gas spectrum. In Table 3.11 the calculated intensity ratio of mass 18, 28, 29, 31 and 32 are seen.

18	28	29	31	32
3,01E-12	2,66E-12	1,28E-11	9,19E-12	5,34E-12

Table 3.10: Absolute intensities

	31
18	0,3274
28	0,2899
29	1,3893
31	1,0000
32	0,5809

Table 3.11: Calculated relative intensities

In Figure 3.6 the calculated methanol fragment (red line) is subtracted from the detected spectrum (black line). The resulting green line shows actual desorption from the sample surface. As can be seen water, carbon monoxide and oxygen show desorption. Formaldehyde however does not desorb. It must be a result of methanol fragmentation in the mass spectrometer.

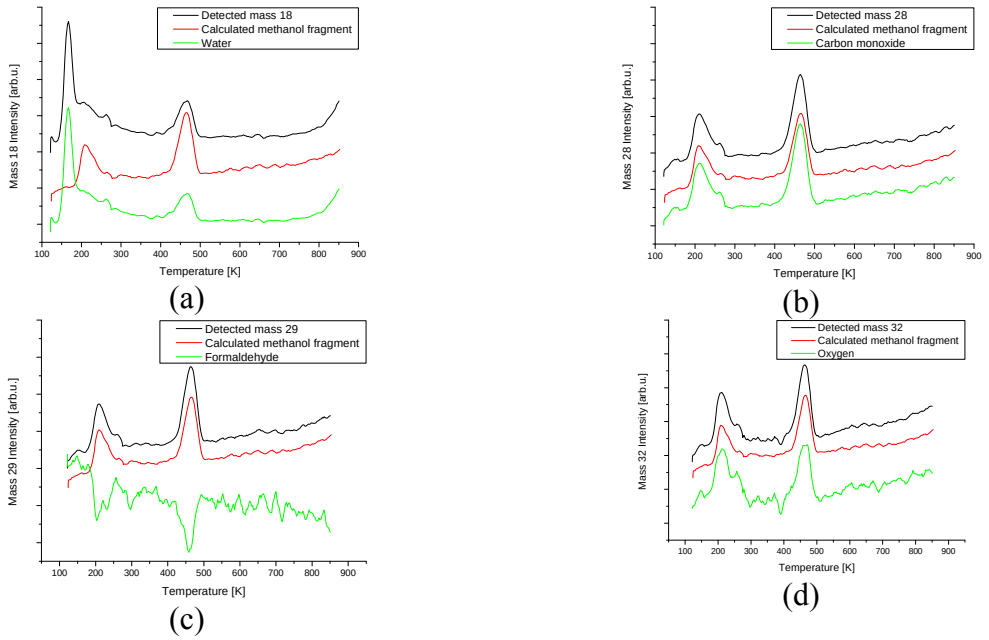

Figure 3.23: Thermal desorption spectra of methanol from Pd/Zn; 0.35 ML zinc, 0.04 L methanol:); (a) mass 18, (b) mass 28, (c) mass 29, (d) mass 32

3.3. Discussion - Methanol desorption from very thin ZnO layers

In the following chapter one representative experiment of each series of experiments was taken to show the different methanol reactions as a result of the production process of the Zn films and the methanol dosage given.

Methanol desorption from three different Pd/ZnO films are compared:

Series 1: Methanol 0.56 L; ZnO 0.35 ML (low oxygen pressure)
Series 2: Methanol 0.56 L; ZnO 0.70 ML (low oxygen pressure)
Series 3: Methanol 0.04 L; ZnO 0.35 ML (low oxygen pressure)

Additionally desorption from a ZnO film above one monolayer (Methanol 1.13 L; ZnO 1.4 ML (low oxygen pressure); chapter 3.1.2) and desorption from a clean Pd (111) surface covered by 1.25 ML methanol and are shown [27].

To make the comparison easier to visualize all spectra of one mass are shown in one plot. It should be noted that the intensities of each single curve must not be compared to the others because their scale was adjusted to fit in the plot.

In Figure 3.24 (a) hydrogen desorption is shown. Clean Pd (Methanol 1.25 ML) shows a clear high temperature desorption peak at 306 K. ZnO covered Pd surfaces show nearly no hydrogen desorption at all. In series two (Methanol 0.56 L; ZnO 0.70 ML (low oxygen pressure)) hydrogen desorption can be seen at 193 K. Thicker ZnO layers (Methanol 1.13 L; ZnO 1.4 ML (low oxygen pressure)) seem to shift hydrogen desorption towards lower temperatures.

Figure 3.24 (b) shows the desorption of water from the sample surface. Series one (Methanol 0.56 L; ZnO 0.35 ML (low oxygen pressure)) shows its peaks at 219 K and 372 K. Series two (Methanol 0.56 L; ZnO 0.70 ML (low oxygen pressure)) and three (Methanol 0.04 L; ZnO 0.35 ML (low oxygen pressure)) have a high temperature peak at 456 K in common. Their low temperature peaks however differ. Series two shows two low temperature peaks one at 152 K and the other at 193 K. The first one is at the exact same position as the peak originating from methanol desorption from clean Pd (Methanol 1.25 ML). A thicker ZnO layer (Methanol 1.13 L; ZnO 1.4 ML (low oxygen pressure)) also shows very similar behavior to Series 3. It shows two low temperature peaks at 141 K and 193 K. Series three shows only one low temperature peak at 167 K. Beyond 800 K water starts to desorb from the sample holder.

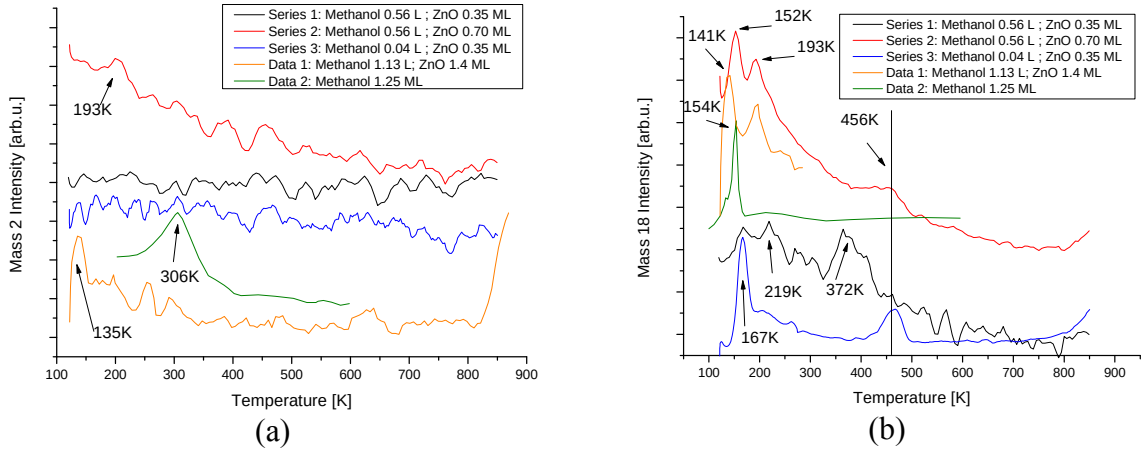

Figure 3.24: Comparison Mass 2 (a) and Mass 18 (b)

In Figure 3.25 (a) carbon monoxide and methanol (fragment) desorption is shown. Series one (Methanol 0.56 L; ZnO 0.35 ML (low oxygen pressure)) desorbs mass 28 similar to mass 18 but in this figure there is a third peak found at 152 K. At this temperature also series two (Methanol 0.56 L; ZnO 0.70 ML (low oxygen pressure)) shows desorption. Furthermore series two shows a second low temperature peak at 193 K just like data 1 (Methanol 1.13 L; ZnO 1.4 ML (low oxygen pressure)) and a high temperature peak at 456 K. At this temperature series three (Methanol 0.04 L; ZnO 0.35 ML (low oxygen pressure)) also shows desorption. Clean Pd (Methanol 1.25 ML) desorbs carbon monoxide about 30 degrees later at 485 K. Series three additionally shows a low temperature peak at 211 K.

Figure 3.25 (b) shows the recorded spectrum of formaldehyde and methanol (fragment). The results are very similar to the ones shown in Figure 3.25 (a), though as can be seen in chapters 3.2.1, 3.2.2 and 3.2.3 detected mass 29 is a result of fragmentation of methanol in the mass spectrometer.

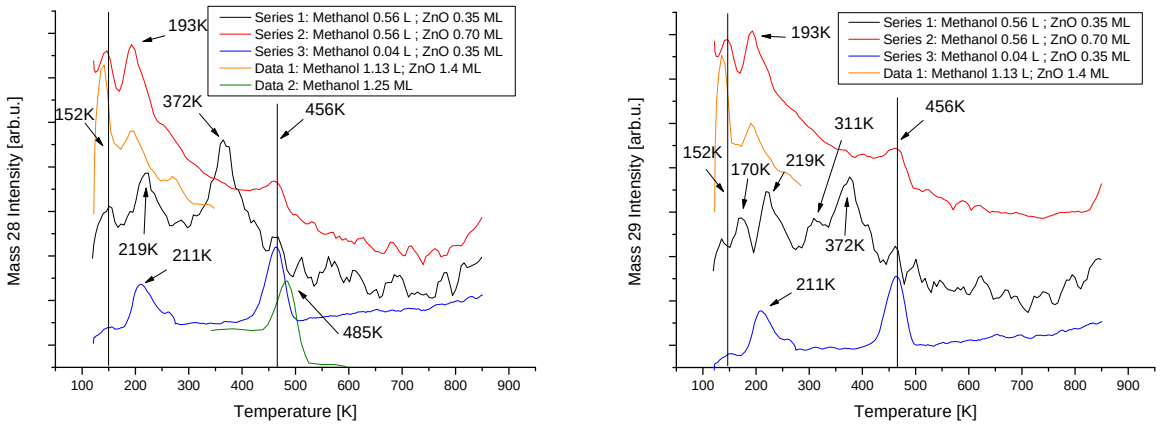

Figure 3.25: Comparison Mass 28 (a) and Mass 29 (b)

In Figure 3.26 (a) methanol desorption is shown. Again results resemble to the ones shown in Figure 3.25 (b) representing formaldehyde and methanol (fragment) desorption. This time the low temperature peak in series one (Methanol 0.56 L; ZnO 0.35 ML (low oxygen pressure)) seems to be shifted even further from 170 K (mass 29) to 175 K (mass 31). The additional fourth peak has also moved from 311 K to 316 K. Desorption from clean Pd (Methanol 1.25 ML) is only seen at very low temperature (127 K). Data one (Methanol 1.13 L; ZnO 1.4 ML (low oxygen pressure)) again shows its two low temperature peaks but no desorption above 250 K.

Figure 3.26 (b) shows oxygen and methanol desorption. The results are very similar to the ones seen in Figure 3.25 (a), representing carbon monoxide and methanol (fragment) desorption. Series one (Methanol 0.56 L; ZnO 0.35 ML (low oxygen pressure)) desorbs mass 32 at 152 K. At this temperature also series two (Methanol 0.56 L; ZnO 0.70 ML (low oxygen pressure)) and data one (Methanol 1.13 L; ZnO 1.4 ML (low oxygen pressure)) show desorption. Furthermore series two and data one show a second low temperature peak at 193 K. Additionally series two shows a high temperature peak at 456 K. At this temperature series three (Methanol 0.04 L; ZnO 0.35 ML (low oxygen pressure)) also shows desorption. A second peak can be seen at 211 K.

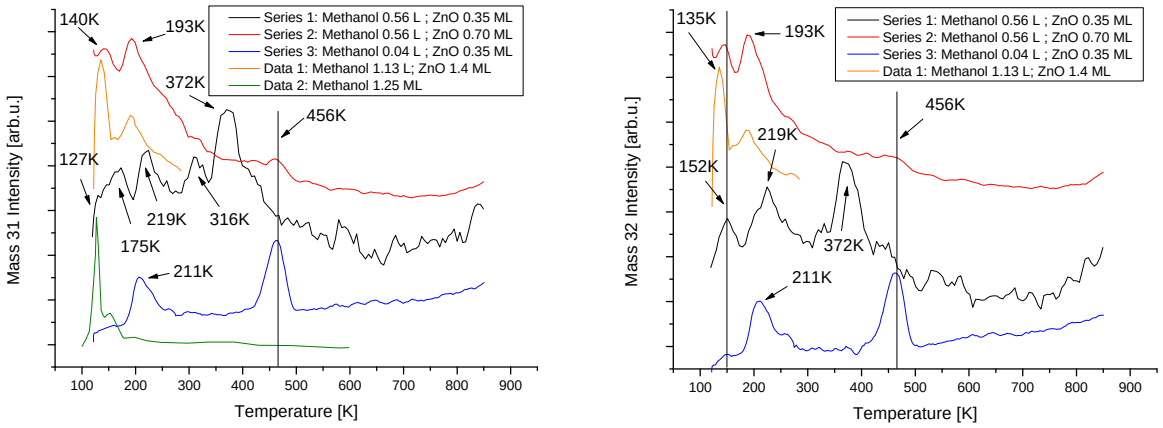

Figure 3.26: Comparison Mass 31 (a) and Mass 32 (b)

In Figure 3.27 (a) desorption of carbon dioxide from the sample surface is shown. Series one (Methanol 0.56 L; ZnO 0.35 ML (low oxygen pressure)) shows one major peak at 372 K. At this temperature also series two (Methanol 0.56 L; ZnO 0.70 ML (low oxygen pressure)) and data one (Methanol 1.13 L; ZnO 1.4 ML (low oxygen pressure)) show desorption. Series three (Methanol 0.04 L; ZnO 0.35 ML (low oxygen pressure)) desorbs carbon dioxide at 251 K. At this temperature series two shows a broad peak with two maxima, one at 210 K and the other at 251 K. Additionally series two shows a peak at 392 K.

Figure 3.27 (b) shows formate desorption from the sample surface. Results are similar to carbon dioxide desorption shown in Figure 3.15 (a). Again series two (Methanol 0.56 L; ZnO 0.70 ML (low oxygen pressure)) shows two major peaks. Both shifted about ten degrees to around 216 K and 403 K. The same result can be seen for formate desorption from 1.4 ML ZnO (Methanol 1.13 L; ZnO 1.4 ML (low oxygen pressure)). Series one on the other hand (Methanol 0.56 L; ZnO 0.35 ML (low oxygen pressure)) desorbs formate at the same temperature as carbon dioxide (372 K). Series three (Methanol 1.13 L; ZnO 1.4 ML (low pressure)) has its desorption maximum of mass 45 at 262 K, which is again ten degrees higher than in mass 44.

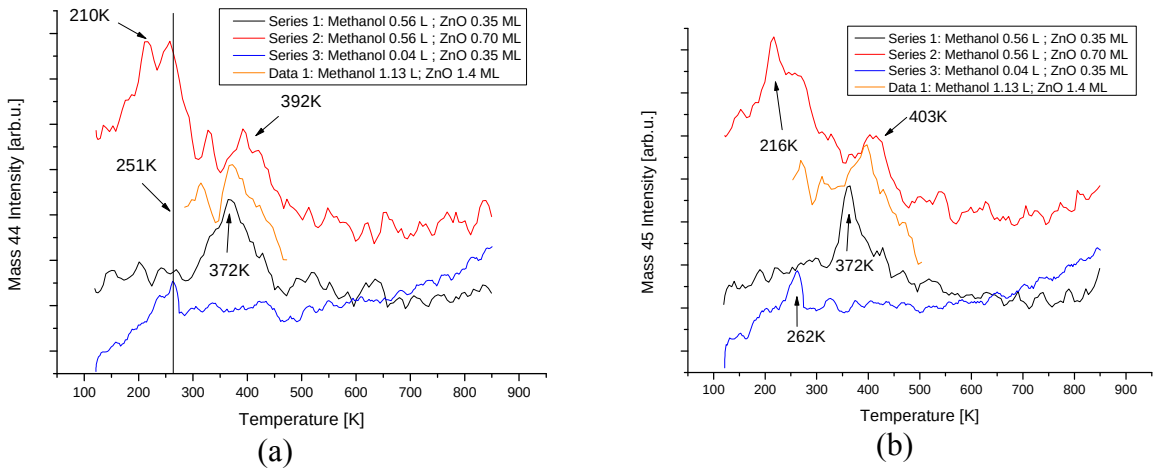

Figure 3.27: Comparison Mass 44 (a) and Mass 45 (b)

In Figure 3.28(a) zinc desorption is shown. All three series from sub monolayer ZnO nearly show the same results, Zinc desorption starts at 916 K which is almost where it is expected to be [5]. ZnO films of more than one monolayer start to desorb Zn at lower temperatures (830 K) which can be explained by lower Zn-Zn binding energies than Zn-Pd [[24], [25], [26]].

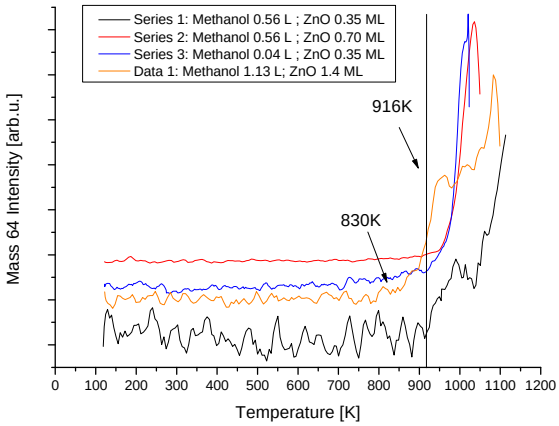

Figure 3.28: Comparison Mass 64

4. IR – study of methanol desorption from Pd/ZnO

In this chapter four series of IR-experiments were done. First methanol on Pd/ZnO (1.4 ML) formed under high oxygen pressure was investigated. Secondly methanol on Pd/ZnO (1.4 ML) formed under low oxygen pressure was explored. In the third series methanol on very thin Pd/ZnO (0.35 ML) formed under low oxygen pressure was investigated. In the fourth series additional IR-measurements after heating the sample to 273 K and 1050 K were done.

4.1. Methanol on Pd/ZnO (high oxygen pressure)

In the first series of experiments methanol on Pd/ZnO formed under high oxygen pressure was investigated. Three different methanol dosages (0.75 L / 1.5 L / 1.88 L) were given.

The sample was cooled down to 123 K to record a first IR-spectrum of clean Pd as a reference after standard cleaning. After that the sample was heated up to room temperature (~300 K) and a film of 1.4 ML ZnO was applied under a high oxygen pressure atmosphere ($1*10^{-5}$ mbar). Then again the sample was cooled down to 123 K to record a second IR-spectrum of Pd/ZnO. After that a dosage of 0.75 L / 1.5 L / 1.88 L methanol was given and subsequently a third IR-spectrum was recorded.

The spectra shown in Figure 4.1 are a result of the third recorded spectrum divided by the Pd/ZnO reference. It shows the change of reflectance of the sample surface after a methanol dosage was given.

As can be seen in Table 4.1 several peaks were found. Experiments with 0.75 L and 1.5 L methanol show clear peaks which can be directly assigned to methanol (2940 cm^{-1}, 2834 cm^{-1}, 1477 cm^{-1}, 1050 cm^{-1}), carbon dioxide (1860 cm^{-1}, 1834 cm^{-1}), formaldehyde (932 cm^{-1}) and formate (2960 cm^{-1}). The third measurement (1.88 L methanol) shows smaller peak intensities but the methanol peaks at 2960 cm^{-1} (CH-stretch) and 2834 cm^{-1} (CO-stretch) are still clearly visible.
This leads to the assumption that methanol gets partly fragmented into CO_2, CH_2O and CO_2H during exposition of the Pd/ZnO surface, which corresponds well with TDS-data as seen in chapter 3.1.2 (Second series of experiments: Pd/ZnO high oxygen pressure).

Wavenumber	*Vibration*	*Compound*	*Source*
2960	CH-stretch	CO_2H	[7]
2940	CH_3-stretch	CH_3OH	[7]
2834	CH-stretch	CH_3OH	[7]
1860	CO_2-stretch	CO_2	[7]
1834	CO_2-stretch	CO_2	[7]
1477	CH_3-deform	CH_3OH	[28]
1050	CO-stretch	CH_3OH	[7]
932	CH_2-wagging	CH_2O	[7]

Table 4.1: Detected wavenumbers and possible compounds

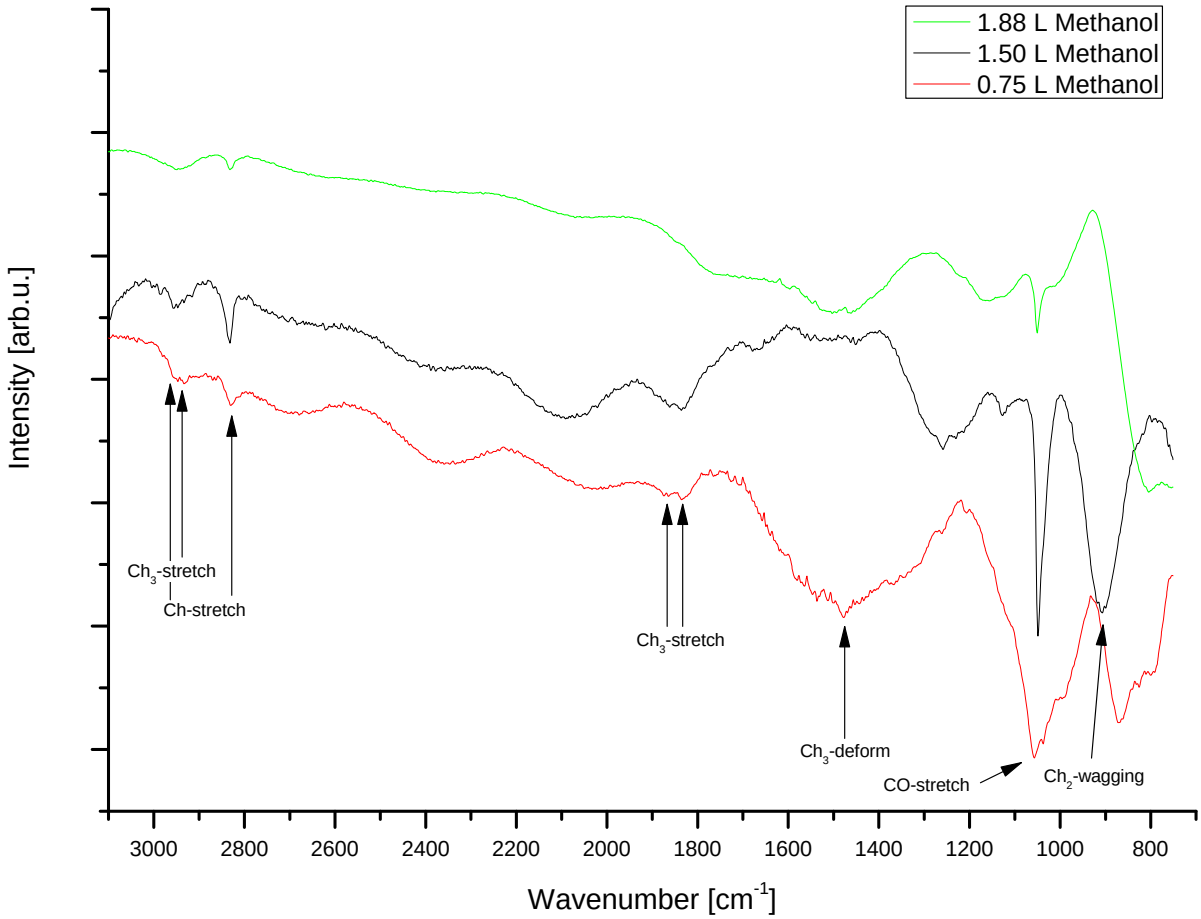

Figure 4.1: Infrared spectrum of methanol on 1.4 ML Pd/ZnO (high oxygen pressure)

4.2. Methanol on Pd/ZnO (low oxygen pressure)

4.2.1. Methanol on Pd/ZnO (1.4 ML)

In the second series of experiments methanol on Pd/ZnO formed under low oxygen pressure was investigated. Three different methanol dosages (0.75 L / 1.5 L / 22.58 L) were given.

The sample was cooled down to 123 K to record a first IR-spectrum of clean Pd as a reference after standard cleaning. After that the sample was heated up to room temperature (~300 K) and a film of 1.4 ML ZnO was applied under a low oxygen pressure atmosphere ($5*10^{-7}$ mbar). Then again the sample was cooled down to 123 K to record a second IR-spectrum of Pd/ZnO. After that a dosage of 0.75 L / 1.5 L / 22.58 L methanol was given and subsequently a third IR-spectrum was recorded.

The spectra shown in Figure 4.2 are a result of the third recorded spectrum divided by the Pd/ZnO reference. It shows the change of reflectance of the sample surface after a methanol dosage was given.

As can be seen in Table 4.2 several peaks were found. The experiments made with 0.75 L and 22.58 L methanol show very similar shaped spectra. They show clear peaks which can be directly assigned to methanol (2940 cm^{-1}, 2834 cm^{-1}, 1473 cm^{-1}, 1048 cm^{-1}, 1028 cm^{-1}), formaldehyde (1257 cm^{-1}, 932 cm^{-1}), formate (2960 cm^{-1}) and water (1510 cm^{-1}). This outcome corresponds to the results shown in chapter 3.1.3 and confirm that detected mass 29 origins from formaldehyde desorption from the sample surface. TDS-data also shows carbon dioxide but it is not found in IR. The third experiment (1.5 L) however differs. Additionally to much smaller intensities it does not show the peaks at 1157 cm^{-1}, 1473 cm^{-1} and 1510 cm^{-1}.

Wavenumber	*Vibration*	*Compound*	*Source*
2960	CH-stretch	CO_2H	[7]
2940	CH_3-stretch	CH_3OH	[7]
2834	CH-stretch	CH_3OH	[7]
1510	bend	H_2O	[7]
1473	CH_3-deform	CH_3OH	[23]
1157	rocking vibration	CO_2 or CH_2O	[7]
1048	CO-stretch	CH_3OH	[7]
1028	CO-stretch	CH_3OH	[7]
932	CH_2-wagging	CH_2O	[7]

Table 4.2: Detected wavenumbers and possible compounds

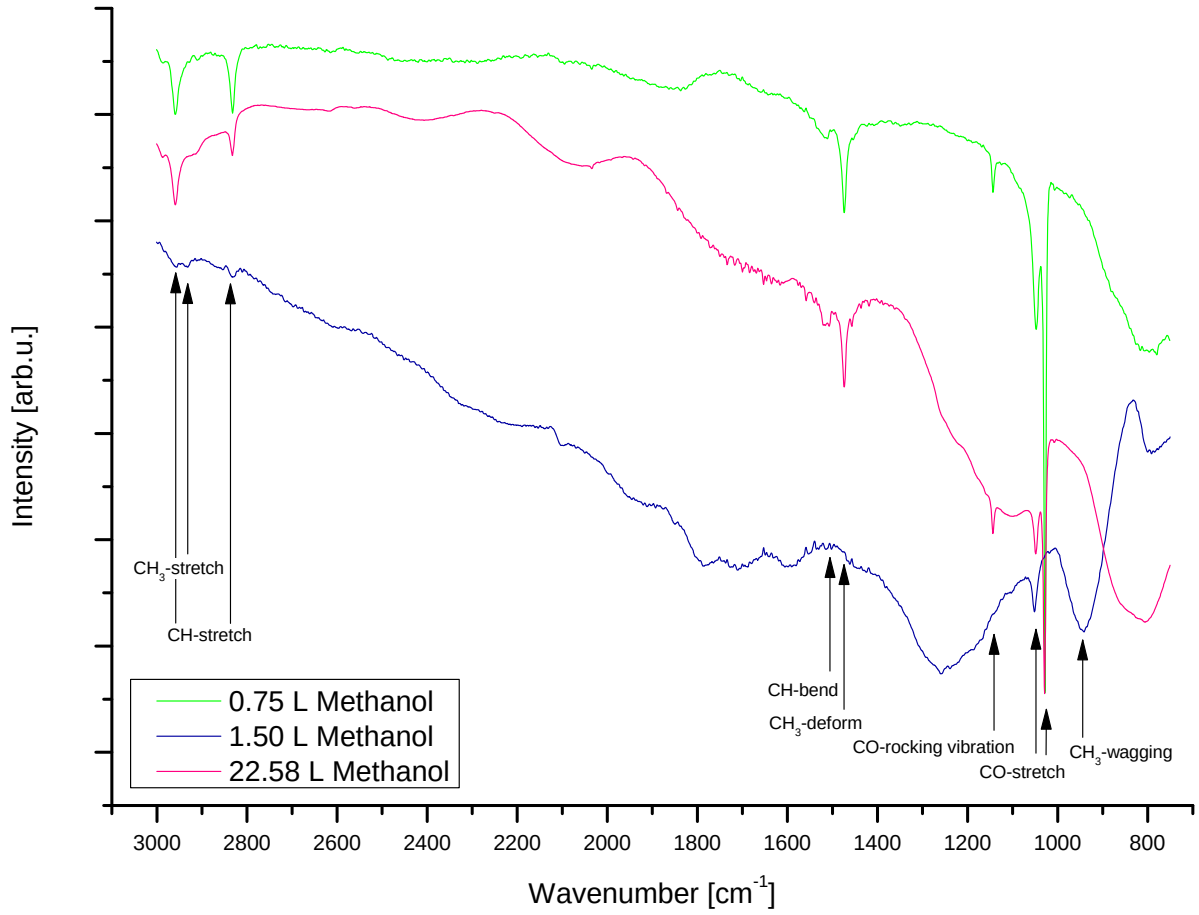

Figure 4.2: Infrared spectrum of methanol on 1.4 ML Pd/ZnO (low oxygen pressure)

4.2.2. **Methanol on Pd/ZnO (0.35 ML)**

In the third series of experiments methanol on Pd/ZnO formed under low oxygen pressure was investigated. Two experiments under the same conditions were done.

The sample was cooled down to 123 K to record a first IR-spectrum of clean Pd as a reference after standard cleaning. After that the sample was heated up to room temperature (~300 K) and a film of 0.35 ML ZnO was applied under a low oxygen pressure atmosphere ($5*10^{-8}$ mbar). Then again the sample was cooled down to 123 K to record a second IR-spectrum of Pd/ZnO. After that a dosage of 0.56 L methanol was given and subsequently a third IR-spectrum was recorded.

The spectra shown in Figure 4.3 are a result of the third recorded spectrum divided by the Pd/ZnO reference. It shows the change of reflectance of the sample surface after the methanol dosage was given.

In Table 4.3 the resulting peaks are shown. Both experiments show similar curve shapes to a large extend. A major difference is seen in the area between 1100 cm^{-1} and 900 cm^{-1} where the first experiment (black line) shows 2 peaks whereas the second experiment (red line) shows only one. These peaks can be directly assigned to methanol (1043 cm^{-1}, 1014 cm^{-1}) and formaldehyde (930 cm^{-1}). This outcome also corresponds to the results shown in chapter 3.2.3 and confirms that detected mass 29 origins from formaldehyde desorption from the sample surface. The absence of peaks showing compounds H_2O, CO, CO_2 and CO_2H which must have been on the sample surface (as they are seen in TDS; page 44), may be a result of the very thin methanol film on the sample surface.
Additional peaks were found at 2260 cm^{-1} and 1940 cm^{-1} but it was not possible to assign them to any possible compound.

Wavenumber	***Vibration***	***Compound***	***Source***
2260		?	
1940		?	
1043	CO-stretch	CH_3OH	[7]
1014	CO-stretch	CH_3OH	[7]
930	CH_2-wagging	CH_2O	[7]

Table 4.3: Detected wavenumbers and possible compounds

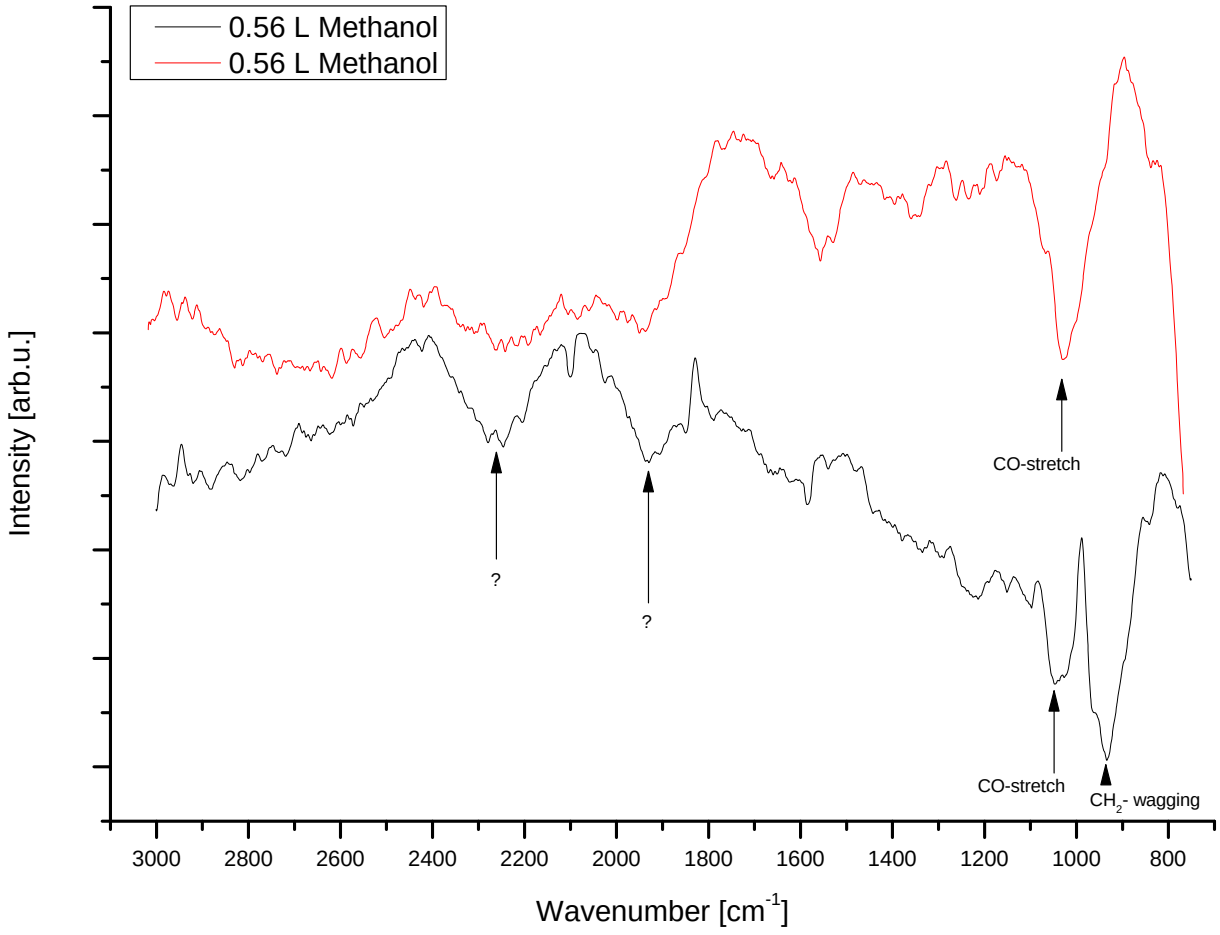

Figure 4.3: Infrared spectrum of methanol on 0.35 ML Pd/ZnO

4.2.3. Methanol on Pd/ZnO (low oxygen pressure) with extra IR-meassurements

In the last experiment the sample was cooled down to 123 K to record a first IR-spectrum of clean Pd as a reference after standard cleaning. After that the sample was heated up to room temperature (~300 K) and a film of 0.35 ML ZnO was applied under a low oxygen pressure atmosphere ($5*10^{-8}$ mbar). Then again the sample was cooled down to 123 K to record a second IR-spectrum of Pd/ZnO. After that a dosage of 0.04 L methanol was given and subsequently a third IR-spectrum was recorded.
To start the TDS measurement the sample was turned to face the QMS. Then it was heated up to ~271 K and immediately cooled down to 123 K. After turning the sample in IR position a fourth IR-spectrum was recorded. Back in TDS position the sample was heated up to ~1000 K and cooled back down to record a last IR-spectrum.

Wavenumber	*Vibration*	*Compound*	*Source*
930	CH_2-wagging	CH_2O	[7]
801	asym. stretch	ZnO	[28]
746	asym. stretch	ZnO	[7]

Table 4.4: Detected wavenumbers and possible compounds

The spectrum shown in Figure 4.4 is a result of dividing the spectra of Pd/ZnO by the reference spectrum of Pd. It shows the change of reflectance by depositing 0.35 ML ZnO on the sample surface. The red marked area is shown in more detail in Figure 4.5. Due to the ultra-thin ZnO and methanol layers only very few significant peaks could be found. In Table 4.4 the detected wavenumbers and possible corresponding compounds are displayed.
Two ZnO peaks are seen at 801 cm^{-1} and 746 cm^{-1}. Additionally one peak is seen at 930 cm^{-1} which may belong to CH_2O. It could be formed during Zn deposition due to hydrogen in the residual gas but this peak does not correspond to the result displayed in chapter 3.2.3 (see page 46). There is shown that measured mass 29 is a result of fragmentation in the QMS.

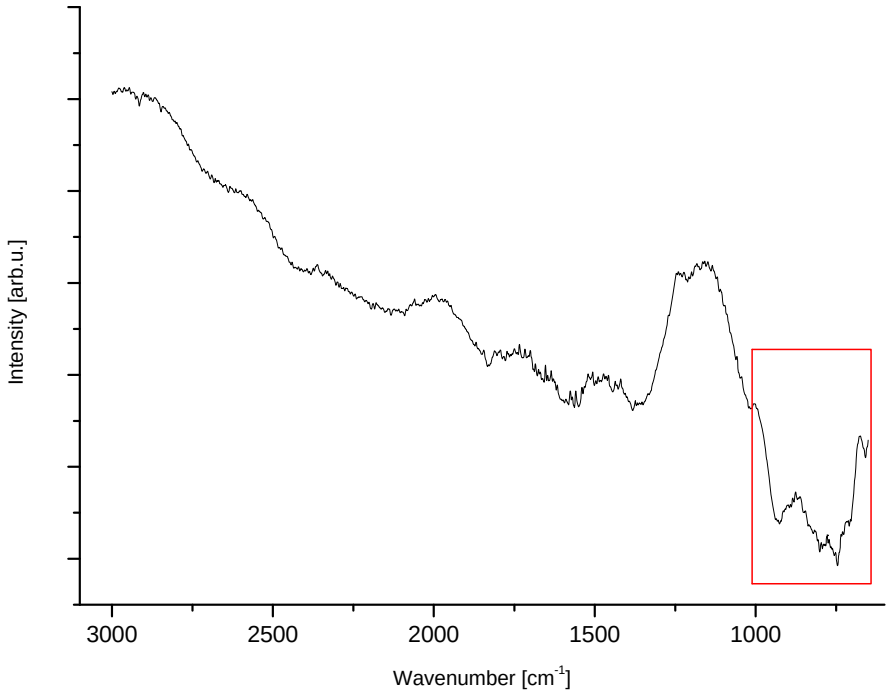

Figure 4.4: Infrared spectrum of 0.35 ML ZnO; overview

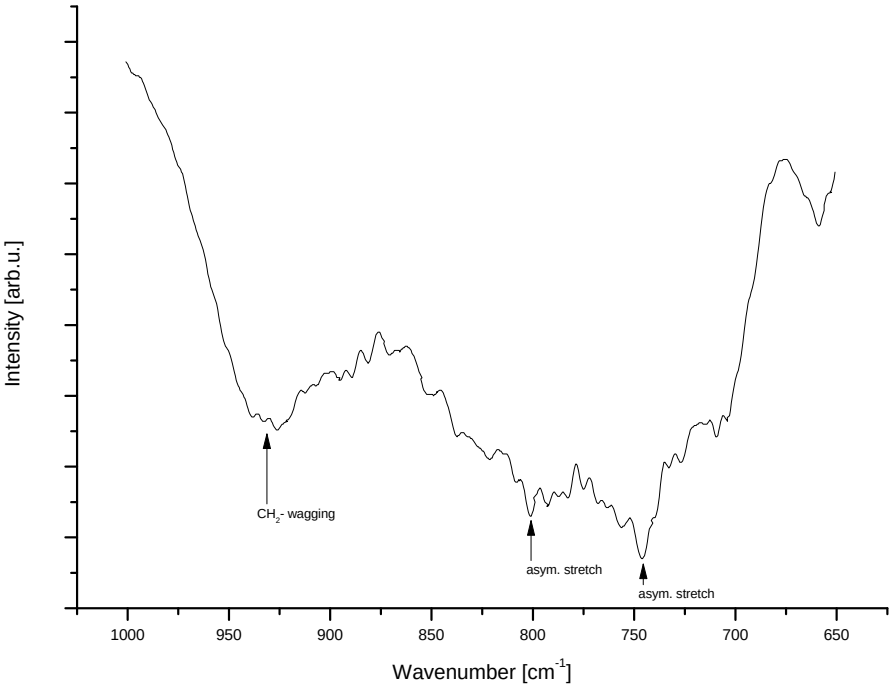

Figure 4.5: Infrared spectrum of 0.35 ML ZnO; detailed view

Figure 4.6 is a result of the third recorded spectrum divided by the Pd/ZnO reference. It shows the change of reflectance after a dosage of 0.04 L methanol was given. In Table 4.5 the detected wavenumbers and possible corresponding compounds are displayed.
Only one peak at 1018 cm^{-1} was found which belongs to methanol. This is the expected outcome after applying a dosage of methanol to the sample surface.

Wavenumber	***Vibration***	***Compound***	***Source***
1018	CO-stretch	CH_3OH	[7]

Table 4.5: Detected wavenumbers and possible compounds

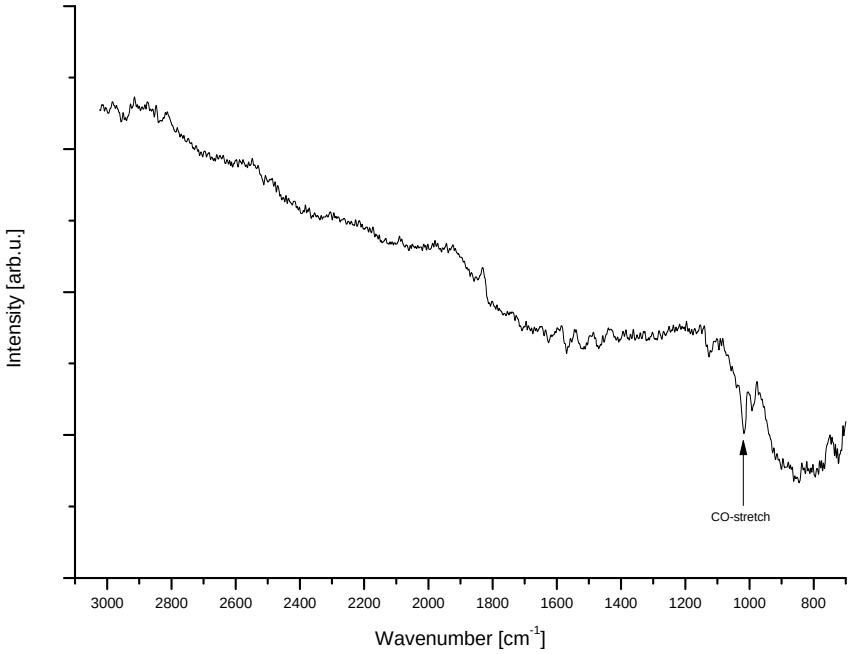

Figure 4.6: Infrared spectrum of methanol before heating

Figure 4.7 is a result of the forth recorded spectrum, taken after the first heating process, divided by the Pd/ZnO reference. It shows the change of reflectance after the sample was heated up to 273 K.
In Table 4.6 the detected wavenumbers and possible corresponding compounds are displayed. A Methanol peak is seen at 997 cm^{-1} which corresponds very well with the results seen in chapter 3.2.3. It shows that methanol desorbs at ~200 K and a second time at 456 K. The same applies to the formaldehyde peak which is found at 1142 cm^{-1}. The detected zinc peak at 817 cm^{-1} also agrees with the TDS-data. Zinc does not desorb until 920 K.

Wavenumber	***Vibration***	***Compound***	***Source***
1142	rocking vibration	CO_2 or CO_2H	[7]
997	CO-stretch	CH_3OH	[7]
817	?	ZnO	[7]

Table 4.6: Detected wavenumbers and possible compounds

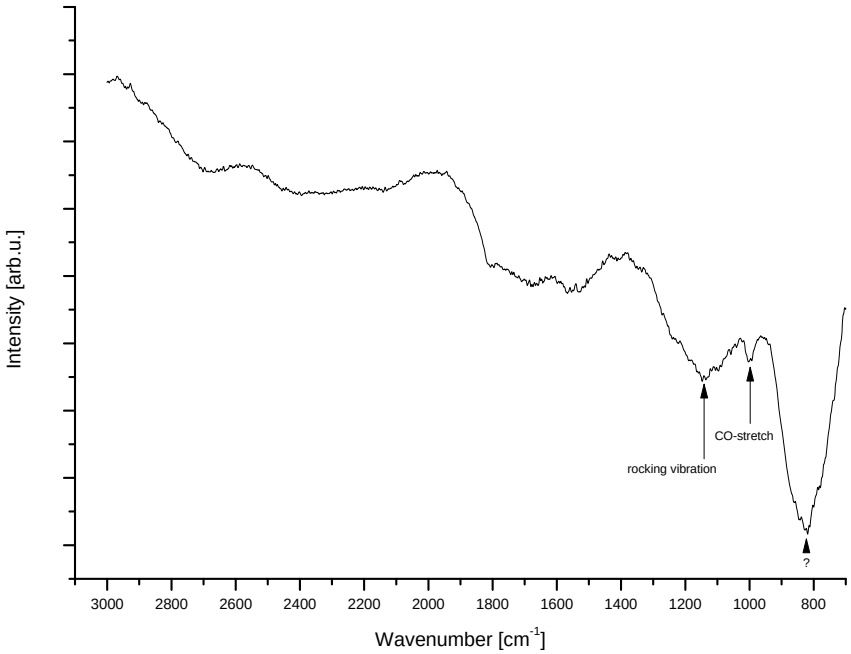

Figure 4.7: Infrared spectrum of methanol (sample heated to 273 K)

Figure 4.8 is a result of the fifth recorded spectrum, taken after the second heating process, divided by the Pd/ZnO reference. It shows the change of reflectance after the sample was heated up to 1050 K.
In Table 4.7 the detected wavenumbers and possible corresponding compounds are displayed. Peaks found at 837 cm^{-1}, 998 cm^{-1}, 1177 cm^{-1}, 1542 cm^{-1} and 1696 cm^{-1} may belong to water, carbon dioxide, methanol and zinc. But after the heating process no compound should be left on the sample surface. One reason for these peaks might be adsorbed residual gas on the sample surface due to the rather long cooling process (about 25 min from 1050 K to 123 K). The other one might be not exactly matching temperatures from the fifth recorded spectrum and the reference spectrum.

Wavenumber	***Vibration***	***Compound***	***Source***
1696	CO_2-stretch	CO_2	[7]
1542	bend	H_2O	[7]
1177	CH_3-rocking	CH_3OH	[28]
998	CO-stretch	CH_3OH	[7]
837	?	ZnO	[7]

Table 4.7: Detected wavenumbers and possible compounds

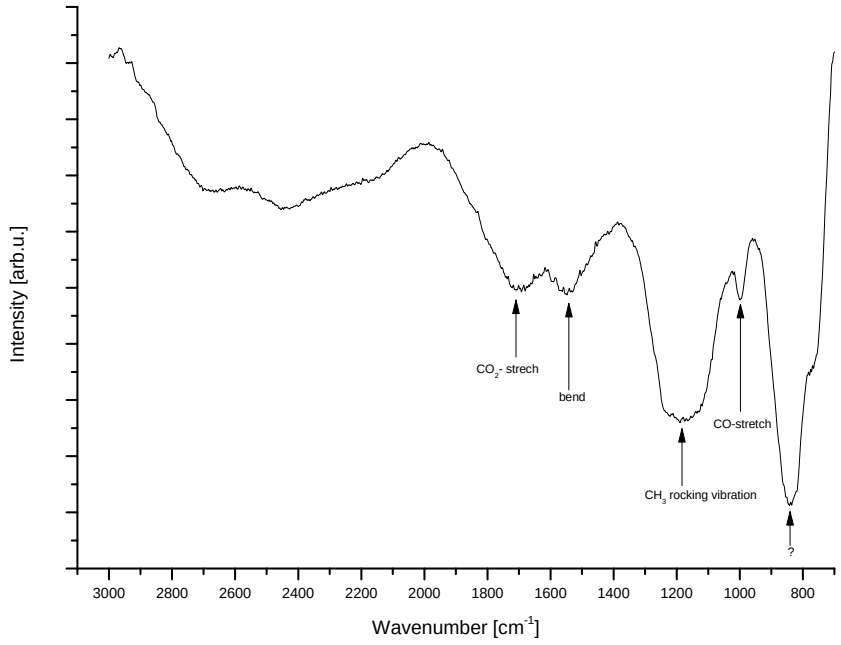

Figure 4.8: Infrared spectrum of methanol (sample heated to 1050 K)

4.3. Discussion

In this chapter methanol on Pd/ZnO was investigated. Chapter 4.1 is dedicated to methanol on Pd/ZnO formed under high pressure whereas chapter 4.2 deals with methanol on Pd/ZnO formed under low oxygen pressure.

In all experiments a CO stretching vibration is seen between 1000 cm^{-1} and 1050 cm^{-1}. This indicates, in the presence of peaks around 2940 cm^{-1} (CH_3 stretching vibration), that methanol was measured on the sample surface.
Another peak seen in all experiments is found around 930 cm^{-1}. It is a result of CH_2 wagging vibrations which are an indicator for formaldehyde. This corresponds well with TDS-data seen in chapter 3 and confirms that detected mass 29 origins from formaldehyde desorption from the sample surface. One exception is found in chapter 4.2.3, where measured mass 29 is only a result of fragmentation in the QMS.

Reducing ZnO and methanol dosage the number of significant peaks found in the spectra becomes significantly smaller. In chapter 4.2.1 (1.4 ML ZnO / 0.75 - 22 L methanol) nine peaks could be found while in chapter 4.2.3, due to drastic dosage reduction (0.35 ML ZnO / 0.04 L methanol), only one peak was detected.
This circumstance makes it very difficult to interpret the obtained IR data from small methanol dosages on ultra-thin ZnO layers.

5. Summary

Within this thesis methanol dissociation and desorption from Pd, Pd/ZnO (formed under low oxygen pressure) and Pd/ZnO (formed under high oxygen pressure) was investigated. Experiments with different ZnO film thicknesses and methanol dosages were done to gain more information about the reaction process in connection to the ZnO thickness and its structure (see chapter 2.4.3).
Compared to the experiments done by F. Weber [7] during his master thesis in the same vacuum chamber, the newly designed sample holder (see chapter 2.2.2), used for experiments done in this thesis, guaranteed stable minimum temperatures and reproducible experimental results (see chapter 3).

In Table 5.1 an overview of TDS results of investigated ZnO surfaces is shown. In Figure 5.1 these results are illustrated. As can be seen the ZnO composition and thickness have a major influence on the reactivity of the sample surface.
Measurement series done with ZnO formed under low oxygen pressure and thinner than 1.5 ML (3.1.3 – 3.2.3) show very similar desorption temperatures. They all desorb mass 18, 28, 29, 31, 32, 44 and 45 at approximately 200 K and a second time at approximately 400 K whereas hydrogen (mass 2) desorption can only be seen at around 200 K.
Series done with ZnO formed under high oxygen pressure (3.1.2) do not show high temperature desorption of mass 18, 28, 29, 31 and 32. Only mass 44 and 45 can be seen at around 350 K.
Experiments done with none oxidized Zn showed a very similar outcome as by obtained reference data from a clean Pd surface [27]. Both desorb mass 18 and 31 at ~160 K, mass 2 at ~310 K and mass 28 at ~470 K.
All experiments showed Zn desorption at about 900 K which is where it is expected to be [5].

RESULTS / TABLE

	0.75 L Methanol 0.2 ML Zinc (no Oxygen)	1.88 L Methanol 1.4 ML ZnO (high pressure)	1.13 L Methanol 1.4 ML ZnO (low Pressure)	0.56 L Methanol 0.35 ML ZnO (low pressure)	0.56 L Methanol 0.7 ML ZnO (low pressure)	0.04 L Methanol 0.35 ML ZnO (low pressure)	1.25 L Methanol clean Pd
H	-- / 306	139 / 188	135 / 196 / --	-- / --	193 / -- / --	200 / --	306
H2O	178 / 461	139 / 188	135 / 196 / 389	219 / 372	152 / 193 / 456	193 / 456	154
CO	178 / 461	139 / 188	135 / 196 / 389	219 / 372	152 / 193 / 456	193 / 456	485
CH2O	178 / 461	139 / 188	135 / 196 / 389	219 / 372	152 / 193 / 456	193 / 456	--
CH3OH	178 / 461	139 / 188	135 / 196 / 389	219 / 372	152 / 193 / 456	193 / 456	127
O2	178 / 461	139 / 188	135 / 196 / 389	219 / 372	152 / 193 / 456	193 / 456	--
CO2	-- / --	348 / --	382 / -- / --	372 / --	210 / 251 / 392	262 / 419	--
CO2H	-- / --	348 / --	397 / -- / --	372 / --	216 / 403 / --	262 / 403	--
Zn	903 / --	877 / --	860 / -- / --	916 / --	920 / -- / --	920 / --	--

Table 5.1: TDS experiments: Detected species and corresponding temperature

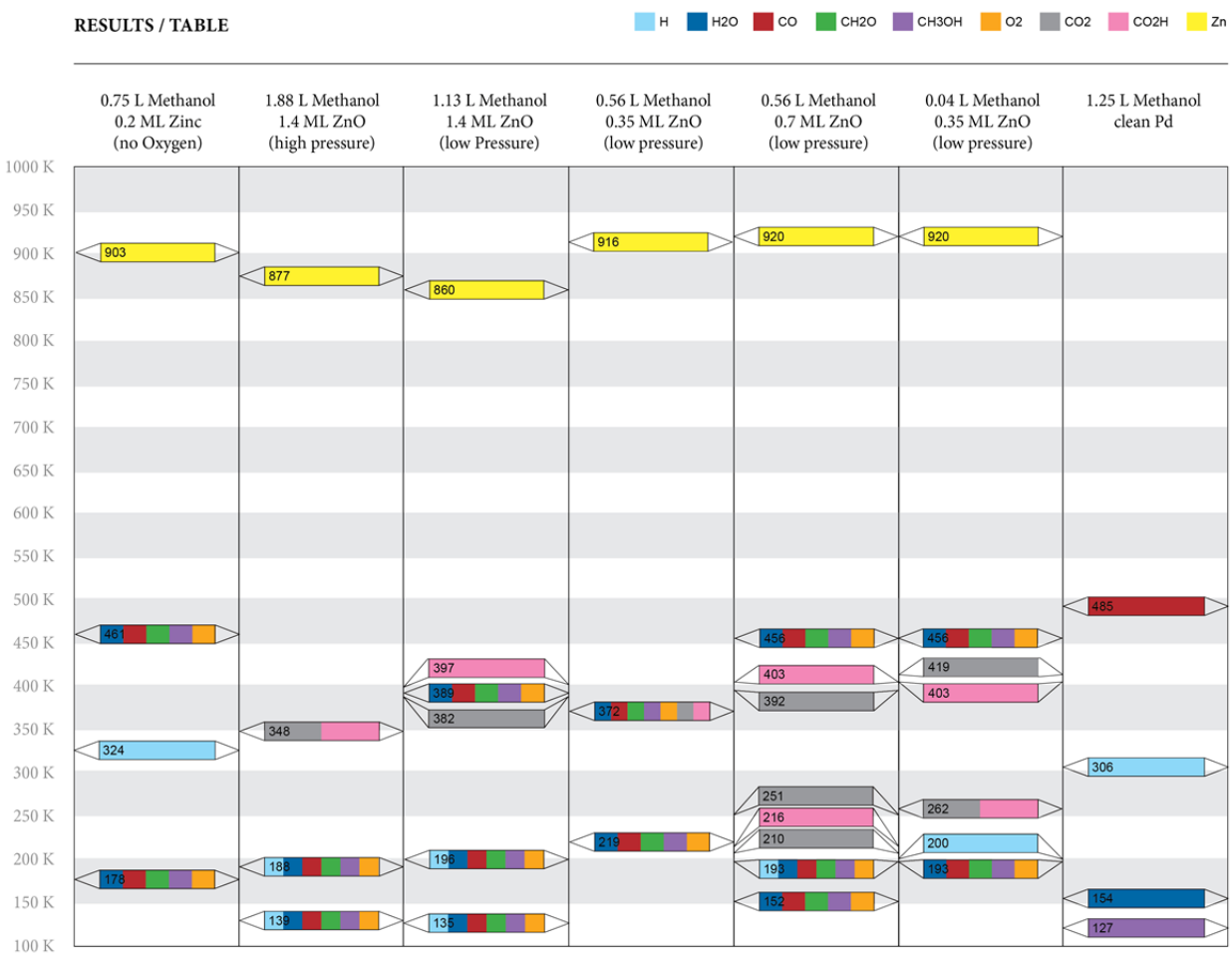

Figure 5.1: TDS experiments: Detected species and corresponding temperature

IR spectroscopy was done to get additional information about the compounds formed on the sample surface during and right after dosing methanol. Measurements were also done in between two heating sessions (3.2.3). In every experiment CO stretching vibration is seen, indicating in the presence of CH_3 stretching vibrations, that methanol was measured on the sample surface. Although IR data is difficult to interpret, the found IR peaks do match the obtained TDS data and additionally support the measured data.

6. Bibliography

[1] A. Casalegno, P. Grassini, and R. Marchesi, "Experimental analysis of methanol cross-over in a direct methanol fuel cell," *Applied Thermal Engineering*, vol. 27, no. 4, p. 748, 2007.

[2] A. Hamnett, "Mechanism and electrocatalysis in the direct methanol fuel cell," *Catalysis Today*, vol. 38, no. 4, p. 445, 1997.

[3] N. Iwasa, T. Mayanagi, W. Nomura, M. Arai, and N. Takezawa, "Effect of Zn addition to supported Pd catalysts in the steam reforming of methanol," *Applied Catalysis A: General*, vol. 248, no. 1, p. 153, 2003.

[4] Z. Chen, K. Neyman, and N. Rösch, "Theoretical study of segregation of Zn and Pd in Pd–Zn alloys," *Surface Science*, vol. 548, no. 1, p. 291, 2004.

[5] H. Gabasch, A. Knop-Gericke, R. Schlögl, S. Penner, B. Jenewein, K. Hayek, and B. Klötzer, "Zn Adsorption on Pd(111): ZnO and PdZn Alloy Formation," *J. Phys. Chem. B*, vol. 110, no. 23, p. 11391, 2006.

[6] Dr. D. Richter, *Gaskinetische Kenngrößen*. Berlin, Germany: Springer Berlin Heidelberg, 2010.

[7] F. Weber, *Reactions of methanol on Pd (111) Pd/Zn- and Pd/ZnO- sufaces*. Graz, 2010, Diploma Thesis.

[8] M. Kratzer, *Reaction Kinetics & Dynamics of H2, O2 and CO on modified Pd(111) surfaces*. Graz, 2009, Dissertation.

[9] P. R. Griffiths and J. A. de Haseth, *Fourier Transform Infrared Spectrometry*. New York, NY [u.a.], USA: Wiley, 1986.

[10] H. P. Koch, *RAIRS investigation of methanol dissociation on Rh and Rh/V surfaces*. Graz, 2004, Diploma Thesis.

[11] A. Rogalski, "HgCdTe infrared detector material: history, status and outlook," *Institute of Physics Publishing*, vol. 68, no. 10, p. 2267, 2005.

[12] C. D. Wagner, W. M. Riggs, L. E. Davis, J. F. Moulder, and G. E. Muilenberg, *Handbook Of X-Ray Photoelectron Spectroscopy*, G.E. Muilenberg, Ed. Minnesota, USA: Perkin-Elmer Corporation, 1978.

[13] (2011, Feb.) Institut Rayonnement Matière Saclay. [Online]. http://iramis.cea.fr/Images/astImg/508_2.jpg

[14] J. B. Pendry, *Low Energy Electron Diffraction*, G. K. T. Conn and K. R. Coleman, Ed. Cambridge, England: Academic Press INC., 1974.

[15] G. Ertl and J. Küppers, *Low Energy Electrons And Surface Chemistry Vol.4*, H. F. Ebel, Ed. Weinheim, Germany: Verlag Chemie, 1974.

[16] (2011, Feb.) Wikimedia. [Online]. http://upload.wikimedia.org/wikipedia/commons/e/e7/LEED_Optics.png

[17] P. E. Miller and M. B. Denton, "The Quadrupole Mass Filter: Basic Operating Concepts," *Journal of Chemical Education*, vol. 36, no. 7, p. 617, 1986.

[18] (2011, Feb.) University of Bristol. [Online]. http://www.bris.ac.uk/nerclsmsf/images/quadrupole.gif

[19] W. Umrath, A. Hermann, A. Bolz, H. Boy, H. Dohmen, K. Gogol, K. Jorisch, W. Mönning, H. J. Mundinger, H. D. Otten, W. Scheer, H. Seiger, W. Schwarz, K. Stepputat, and D. Urban, *Grundlagen der Vakuumtechnik*, Lybold, Ed. Köln, Deutschland, 1997.

[20] Varian, *Ionisation Gauge Instruction Sheet Models UHV-12-K, UHV-12-KF, UHV-24, UHV-12-P*, Varian, Ed. Pao Alto, USA, 1977.

[21] W.H. Weinberg and C.-M. Chan, "An Analysis Of Thermal Desorption Mass Spectra II," *Applications of Surface Science*, p. 377, 1978.

[22] W.H. Weinberg and C.-M. Chan, "An Analysis Of Thermal Desorption Mass Spectra I," *Applications of Surface Science 1*, p. 360, 1978.

[23] P. A. Redhead, "Thermal Desorption of Gases," *Vacuum*, vol. 12, no. 4, p. 203, 1962.

[24] H.P. Koch, I. Bako, G. Weirum, M. Kratzer, and R. Schennach, "A theoretical study of Zn adsorption and desorption on a Pd(111) substrate," *Surface Science*, vol. 604, no. 11-12, p. 926, 2010.

[25] G, Weirum, M. Kratzer, H. P. Kock, A. Tamtögl, J. Killmann, I. Bako, A. Winkler, S. Surnev, F. P. Netzer, and R. Schennach, "Growth and Desorption Kinetics of Ultrathin Zn Layers on Pd(111)," *Journal of physical chemistry. C*, vol. 113, p. 9788, 2009.

[26] G. Weirum, C. Barcaro, A. Fortunelli, F. Weber, R. Schennach, S. Surnev, and F. P. Netzer, "Growth and Surface Structure of Zinc Oxide Layers on a Pd(111) Surface," *Journal of physical chemistry. C*, vol. 114, no. 36, p. 15432, 2010.

[27] J.-J. Chen, Z.-C. Jiang, Y. Zhou, B.R. Chakraborty, and N. Winograd, "Spectroscopic studies of methanol decomposition on Pd[lcub]111[rcub]," *Surface Science*, vol. 328, no. 3, Apr. 1995.

[28] National Institute of Standards and Technology. (2011, May) NIST Chemistry WebBook. [Online]. http://webbook.nist.gov/chemistry/

[29] C. Lingg. (2011, Mar.) Wikipedia. [Online]. http://de.wikipedia.org/wiki/Brennstoffzelle

[30] Specs, *ErLEED User Manual*, 13th ed. Berlin, Germany: Specs GmbH, 2003.

7. List of Figures

8. Appendix

Calculation of Pd surface atoms:

Surface of Pd crystal:

$$A = 0.5^2 \cdot \pi = 78.53 mm^2 \quad \textbf{(8.1)}$$

Lattice constant of Pd:

$$a = 3.95 Å \quad \textbf{(8.2)}$$

Calculating the distance to the nearest neighbor in an fcc lattice:

$$R = \frac{\sqrt{2}}{2} a = 2.79307 Å \quad \textbf{(8.3)}$$

Calculating the number of surface atoms:

$$\frac{A}{\left(R \cdot 10^{-7}\right)^2} = 1.0066 \cdot 10^{15} \quad \textbf{(8.4)}$$

Temperature-measurement-error

The measurement error is calculated with help of Figure 8.1. It shows the primary peak which is a result of desorption from the tantalum wires. Desorption should always take place at the same temperature. But as can be seen in Figure 8.1 the peak position shifts from experiment to experiment. This fact is used to estimate the temperature-measurement-error to $\Delta T = \pm 10°$.

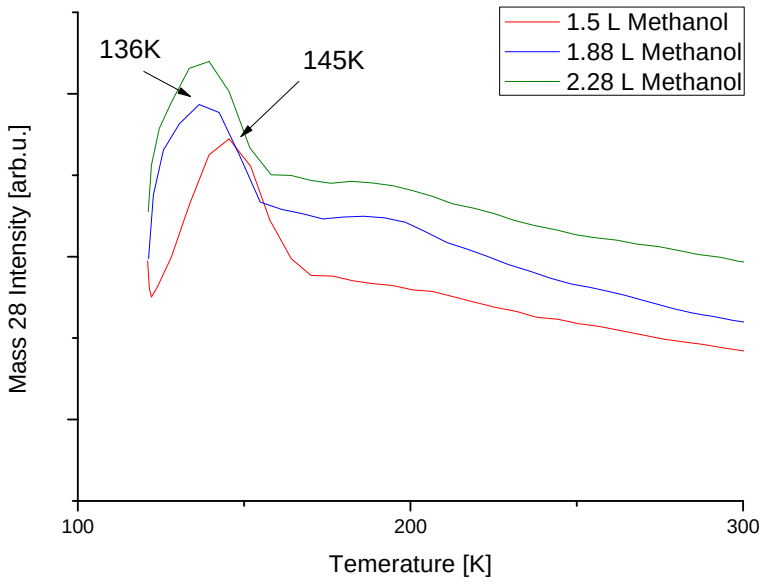

Figure 8.1: TDS spectrum of Mass 28